Groundwater age as an indicator of nitrate concentration evolution in aquifers affected by agricultural activities

Brkić, Željka; Larva, Ozren; Kuhta, Mladen

Groundwater age as an indicator of nitrate concentration evolution in aquifers affected by agricultural activities

Željka Brkić*, Ozren Larva & Mladen Kuhta

Croatian Geological Survey, Department of Hydrogeology and Engineering Geology, Sachsova ulica 2, 10000 Zagreb, Croatia

* Corresponding author: Željka Brkić zeljka.brkic@hgi-cgs.hr

Abstract

The western part of the Drava alluvial aquifer system, located in northern Croatia, contains significant amounts of groundwater, which is primarily used for public water supply and irrigation. The groundwater of this system contains high concentrations of nitrate which is why aquifer system is classified as a groundwater body of poor chemical status under the Water Framework Directive (WFD).

We investigated the groundwater age in this aquifer system and compared the nitrate concentrations in groundwater and the nitrogen pressure from agricultural activity with respect to the estimated mean groundwater age. We used a combination of the environmental tracers: chlorofluorocarbons (CFCs: CFC-12, CFC-11, and CFC-113), sulphur hexafluoride (SF_6), tritium (^3H) and noble gases. By applying lumped parameter models, we determined the groundwater age in aquifers at different depths. On comparing the recharge year, historical data on nitrate concentrations in groundwater, and nitrogen pressure from agricultural activity, we found that these elements are closely related. Our investigation was also supported by the results of numerical simulation of the evolution of nitrate concentration in the saturated zone of the aquifer. The decrease in agricultural pressure caused a decrease in the nitrate concentrations in the youngest, shallow, and oxic groundwater. However, the trend of increasing nitrate concentrations in the deeper part of the aquifer can last for many years. Our research supports the thesis that groundwater age is an important criterion for assessing the

effectiveness of protection measures taken in groundwater management and implementation of the WFD and Nitrate Directive.

Keywords: porous media, groundwater age distribution, nitrogen pressure, agriculture, nitrate concentration trend, modelling

1. Introduction

For sustainable groundwater management, it is vital to have a comprehensive understanding of the complex and diverse processes of groundwater recharge and the processes that occur during groundwater flow. There is a large number of terms and phrases in literature on groundwater which refer to the age and lifetime of a groundwater molecule. For instance, the groundwater age represents the time taken by a water molecule to reach a specific location, for such as an observation well, from the moment it was recharged into the subsurface system (Kazemi et al., 2006). The groundwater residence time is another commonly used term and represents the time taken by water particles to travel from the recharge area to an aquifer discharge area, such as a river or spring (Modica et al., 1998). Suckow (2014) provides basic definitions such as the idealised age as one that corresponds to the results of particle tracking and piston flow model of groundwater flow, mean residence time involving an age distribution, and apparent age. The idealised groundwater age is the time taken by water to travel from groundwater table to the sampling site (Torgersen et al., 2013, Suckow, 2014). This definition is suitable for groundwater age dating methods based on dissolved gases (such as $^{3}H/^{3}He$, chlorofluorocarbons (CFCs), and sulphur hexafluoride (SF_6)) because it is a measure of the time elapsed since the water was last in contact with the atmosphere. Age is generally determined by matching the measured concentration of dissolved gases in the sample with the corresponding input concentration of the same gases in a given year of recharge. In nature, the occurrence of various physical and chemical processes affects the concentrations of dissolved substances in the aquifer; hence, the groundwater age, estimated using concentrations of dissolved substance, is not necessarily equal to the time of water transport. In principle, the accuracy of a particular groundwater age depends

on how these substances are carried by water. The concentrations of all solutes are, to some extent, influenced by the transport processes. Their concentrations can be affected by chemical and physical processes during transport, such as degradation, sorption, diffusion, and dispersion. Therefore, it is important to understand that the age of groundwater determined from the concentrations of these tracers actually represents the age of the tracers.

The concept of residence time is independent of the definition of idealised age (Suckow, 2014). In natural groundwater systems, the residence time depends on the position of the water molecule in the catchment area. For example, the residence time in a gravel layer of high hydraulic conductivity will vary from the residence time in a clay layer with low conductivity. Considering the residence times in an actual aquifer system, it is clear that the water samples represent a mixture of idealised ages. The mean for a mathematically defined mixture of different idealised ages can be calculated using lumped parameter models (LPMs). Each of such models exhibits its own age distribution curve. For groundwater management, the shape of the age distribution in these models is more significant than the actual mean value (Suckow, 2014). For some tracers or tracer combinations, such as ^{14}C and $^{3}H/^{3}He$, the sample age can be derived using a mathematical formula; Suckow (2014) suggests using the term ‘apparent tracer age’ to denote the age derived from this method.

Groundwater age data can help estimate not only the recharge area, flow path and amount of groundwater that can be used sustainably, but also the lag of groundwater in relation to a pollution event, and expected future pollution discharged into groundwater bodies (e.g. Visser, 2009). Groundwater quality generally improves with a time lag from the cessation of pollution input. The extent of improvement depends on the type of pollution. In the case of groundwater pollution by nitrates that are relatively stable in an oxic environment, which is characteristic of the study area, the duration of poor groundwater quality primarily depends on the mean age of groundwater from the cessation or reduction of nitrate input. Considering this, groundwater age is becoming an important tool for assessing the effectiveness of protection measures.

78 Nitrate leaching into groundwater is a major source of pollution caused by intensive agriculture.
79 Studies conducted in many countries have found that the measured nitrate concentrations are closely
80 related to agricultural practices (Broers & van der Grift, 2004; Lindsey et al., 2003; Cambray et al.,
81 2005; Stockmarr et al., 2005; Seifert et al., 2008; van Grinsven et al., 2016). Furthermore, it was
82 reported that the protection measures applied in agricultural production in Denmark have affected
83 nitrate concentrations in groundwater (Hansen et al., 2012, 2017).

84 The analysis of the effectiveness of protection measures and trends was primarily considered with
85 regard to the impact of agricultural production on increased nitrate concentrations in groundwater.
86 This is because increased nitrate concentrations in groundwater are the among the most pressing
87 environmental concerns in many countries. A review of the status of the environment and the
88 consequences of the time lag of nitrate concentrations in groundwater in relation to the time of
89 application of measures and the load from agricultural production in Europe and North America led
90 to the conclusion that a water protection policy, aimed at reducing or preventing nitrate pollution in
91 water, must take into account the time lag of groundwater and the transport of solutes through the
92 unsaturated and saturated zone (Vero et al., 2018). This lag must be quantified in order to establish
93 realistic deadlines, thresholds, and expectations, and to plan effective water management practices.
94 In this regard, it is necessary to determine the groundwater age, that is, the groundwater residence
95 time, of groundwater polluted by nitrates, in which the measured nitrate concentrations can be related
96 to the historical input of nitrogen into groundwater. Thus, the reversal trend in agricultural pollution,
97 as required by the European Union Water Framework Directive (WFD), can be demonstrated, or the
98 effects of implemented protection measures on nitrate reduction in groundwater can be assessed
99 (Visser et al., 2009).

100 The study area represents intensive agricultural areas: a combination of mostly (85%) crop
101 production, intensive vegetable production, and livestock breeding (Bubalo et al., 2014).
102 Additionally, there are many cattle and chicken farms. High-value, intensively managed crops, such
103 as vegetables and other irrigated agricultural crops, to which large amounts of nitrogen fertiliser are

usually applied, can significantly contribute to nitrate contamination of surface and groundwater (Bubalo et al., 2014). The application of organic fertilisers (manure) additionally contributes to nitrate leaching. Higher rates of nitrate losses were recorded in manure treatment than in compost and inorganic N treatments (Basso & Ritchie, 2005; Thomsen, 2005). Groundwater quality and quantity monitoring in the Varaždin area has been conducted on an ongoing basis for several years. It has been observed that the groundwater is oxic and has high nitrate concentrations which are associated with agricultural production and intensive application of fertilisers and manure; nitrate concentrations have been increasing in groundwater since the 1970s, and a trend reversal has been achieved in the last 15 years.

This paper provides for the first time a comprehensive assessment of the dependence of nitrate concentration in groundwater on agricultural activity in Croatia. We investigated the groundwater age in this aquifer system and compared the nitrate concentrations in groundwater with the nitrogen pressure from agricultural activity with respect to the groundwater age. The atmospheric trace gases CFC-11, CFC-12, CFC-113, and SF_6, as well as the radioactive isotope of hydrogen, tritium, and its product, helium-3, were used for the groundwater age estimation. The production of CFCs started in early 1940s. Its concentrations gradually began to decrease after the adoption of the Montreal Protocol in the second half of the 1980s. However, the concentration of SF_6 is still increasing. The high ^3H concentrations in the atmosphere were consequences of thermonuclear tests, which began in 1952; peak concentrations of ^3H in rainfall were recorded in 1963 and 1964. The data over the last 20 years suggest a nearly constant mean annual ^3H concentration (Dulinski et al., 2019; Krajcar Bronić et al., 2020). We employed the LPM to determine the groundwater age in aquifers at different depths. By comparing the recharge year, historical data on nitrate concentrations in groundwater, and nitrogen pressure from agricultural activity, we found that they are closely related to each other. These findings were supported by the results of numerical simulations of the evolution of nitrate concentrations in the saturated zone of the aquifer.

2. Case study

The Varaždin area is located in the valley of the Drava River at an altitude of 170–200 m above sea level. It is bounded to the north by the Drava River and to the west and south by mountainous areas. The valley is dominated by arable land and meadows. The largest settlement in the area is the city of Varaždin. In the wider study area, two hydroelectric power plants are built on the Drava River with associated inflow channels, accumulation lakes, engine rooms, and drainage canals (Fig. 1).

Fig. 1.

According to Köppen's classification of climate types, the Varaždin area belongs to the Cfb climate type (Šegota & Filipčić, 1996). It has a moderately warm, humid climate with warm summers. The mean annual air temperatures for the periods 1960–1991 and 1971–2000 were 9.9 °C and 10.2 °C, respectively (Zaninović et al., 2008). The average annual rainfall for the same period was 879.2 and 843.1 mm, respectively.

The Varaždin area is composed of Quaternary sediments within which an alluvial aquifer of intergranular porosity is formed (Figs. 1, 2). The lithological composition of the aquifer is dominated by gravel and sand with subordinate silt and clay contents. In the westernmost part of the area, the hydraulic conductivity of the aquifer reaches 300 m/day (Larva, 2008). It gradually decreases downstream, approximately reaching 170 m/day in the area east of the Bartolovac pumping site (Fig. 1). The thickness of the aquifer increases from west to east (Fig. 2). The aquifer is covered by a thin, occasionally absent layer of semipermeable deposits, allowing high amounts of precipitation infiltration, but also increasing vulnerability of groundwater to pollution by a high degree. The aquifer is unconfined. In hydrogeological terms, a semipermeable interlayer (aquitard) divides the aquifer into an upper and a lower aquifers. This aquitard of regional importance appears in the vicinity of Varaždin and extends further downstream. It is composed of silt and clay with a high sand content and a thickness of a few meters. However, the layer is occasionally absent.

Fig. 2.

Groundwater recharge in the study area is mainly achieved through rainfall infiltration. The recharge rates are relatively high and range from 20% to 30% of annual precipitation, depending on the thickness and permeability of the covering layer and type of land use (Urumović et al., 1981; Patrčević, 1995; Brkić, 1999). The Drava River is in direct contact with the aquifer and drains groundwater under natural conditions. The construction of the hydroelectric power plants on the Drava River altered the natural conditions; consequently, the aquifer is recharged in the vicinity of the accumulation lakes, while the drainage canals intensively drain the groundwater (Fig. 1).

3. Data and methods

In our approach, four input variables (hydrogeological data, historical groundwater quality data, historical pressure from agriculture data, and environmental tracers) were selected, and then evaluated and processed. The interrelation between individual segments of the research is shown in Fig. 3.

Fig. 3.

3.1.Groundwater sampling for CFCs and SF_6 analyses

Groundwater sampling was conducted during two periods: 2017–2018 and 2019–2020 (Table 1). Eight samples were collected from the observation boreholes at three depths (Table 1). All samples were collected with a submersible pump Grundfos MP1. Prior to sampling, at least three borehole volumes of water were pumped out with a pumping rate of about 0.4 L/s. After reaching stable conditions for temperature, electrical conductivity, and pH, groundwater samples were collected in a 'low-flow' regime with a pumping rate of ~1 L/min.

Samples for the analyses of CFCs and SF_6 were collected following the methods described by Oster et al. (1996). Samples were collected in 500-mL glass bottles stored in containers filled with the same water to prevent contamination. Groundwater samples were collected in 1-L high density polyethylene bottles for analyses of ^3H, and in copper tubes with a volume of ~ 40 mL for analyses

of noble gases, as described by Weiss (1968). After purifying the copper tubes with at least 10 volumes of tubing, the copper tubes were sealed at both ends with clamps.

Table 1

3.2.Groundwater quality data

Groundwater quality monitoring data were collected from the national monitoring database for which the Hrvatske vode (a legal entity for water management in Croatia) is responsible, and from the groundwater quality databases in the investigated recharge areas of the pumping sites (Table 2).

Table 2

3.3.*Analysis of CFCs and $^{3}H/^{3}He$*

Analyses of CFCs and SF_6 were performed in Spurenstofflabor (Wachenheim, Germany) using gas chromatography, following the methods described by Oster et al. (1996). Tritium and noble gases were analysed in Isotoptech Zrt. (Debrecen, Hungary). The samples were measured using a Helix SFT and a VG5400 noble gas mass spectrometer and were determined using the method described by Palcsu et al. (2010).

3.4.Groundwater age assessment methods

Groundwater age dating using the atmospheric trace gases is based on Henry's law of solubility. Using this method, the historical date at which a parcel of water was recharged to a groundwater system can be calculated. A notable assumption is that, at this point, the water samples were at equilibrium with the gas concentration in the unsaturated zone. The procedure applied for converting the measured concentrations in groundwater samples, expressed in picomol per liter (pmol/L) or femtomol per liter (fmol/L), to the atmospheric equivalent concentration (EAC), expressed in parts

per billion per volume (pptv), is described in Kazemi et al. (2006) and IAEA (2006). A recharge elevation of 200 m and a recharge temperature of 10 °C (Table 2), as well as a groundwater salinity of 500 mg/L were used. The physical and chemical properties of CFCs were taken from Kazemi et al. (2006), Cook and Herczeg (2000), Bu & Warner (1995), Cook and Solomon (1995), Warner & Weiss (1985), and for SF_6 from Cosgrove and Walkley (1981). The obtained EAC values were then compared to the graphs of CFC concentrations in the air in the Northern Hemisphere (https://water.usgs.gov/lab/software/air_curve/index.htm), and the year when the analysed CFCs infiltrated into the groundwater via precipitation was determined (groundwater recharge).

To perform groundwater dating with the sparingly soluble SF_6 tracer, excess air must be considered (Kazemi et al., 2006, Chambers et al., 2019). For the majority of groundwater systems, the excess air is in the range of ~1–3 cm^3/L at standard temperature and pressure (STP) (Blusemberg & Plummer, 2000). According to the graph which displays the correction factors for excess air as a function of recharge temperature (Chambers et al., 2019), the excess air correction factor for SF_6 was assumed to be 0.8, which corresponds to ~2 cm^3/L at an STP; the CFC concentrations were not corrected. The advantages and disadvantages of groundwater dating with CFCs and SF_6 are described in Goody et al. (2006), Kazemi et al. (2006), and Chambers et al. (2019). Busenberg and Plummer (2000) considered that the SF_6 method is useful for dating very young groundwater and recharge in urban environments where CFCs can be elevated owing to local anthropogenic sources.

In groundwater younger than the mid-1960s, the highest concentrations of ^3H can no longer be registered due its radioactive decay into ^3He. However, the apparent age of groundwater can be calculated from the $^3H/^3He$ ratio in a groundwater sample (Schlosser et al., 1988, 1989; Solomon et al., 1992, 1993; Tolstikhin & Kamenskiy, 1969). ^3H input refers to the ^3H concentration which enters the saturated zone at the time of recharge. Assuming piston flow conditions, the output represents the sum of ^3H and $^3He_{(trit)}$ in the sample. The historical ^3H data for precipitation at the Vienna, Ljubljana and Zagreb Global Network of Isotopes in Precipitation (GNIP) stations were analysed as input data for ^3H.

Groundwater ages were also calculated using LPMs (Maloszewski and Zuber 1996) which are useful for describing groundwater systems with a small number of parameters (Maloszewski et al., 1992, 2002). LPMs are the simplest and most convenient for systems limited to one or two parameters, containing young water and concentrations of "modern" tracers such as seasonally variable ^{18}O, ^{2}H, ^{3}H, ^{85}Kr, CFCs, and SF_6 as input variables (Maloszewski & Zuber, 1996). In this study, CFC and SF_6 data inputs were presented as their atmospheric mixing ratios in precipitation for the Northern Hemisphere atmosphere. The historical ^{3}H data for precipitation at the Vienna, GNIP station were used as input data for ^{3}H.

The LPMs are represented mathematically as residence time distribution functions or age distribution functions *[g(t)]* (Maloszewski and Zuber, 1982). A water sample is considered to be composed of many parcels with various flow paths leading to the sampling site. Each parcel represents a relatively discrete groundwater age and tracer concentration. Mathematically, all LPMs for steady-state flow systems with a time-variable tracer input are convolution integrals, as follows:

$$C_{out}(t) = \int_{-\infty}^{t} C_{in}(t') \cdot g(t-t') \cdot e^{-\lambda(t-t')} dt' \quad (1)$$

where C_{out} is the output tracer concentration in groundwater (well, borehole, or spring), C_{in} is the input tracer concentration in the system, t is the sampling date, t' is the entry time into the system, and $g(t-t')$ is the residence time distribution or the age distribution function. The term $e^{-\lambda(t-t')}dt$ is related to radioactive decay. The terms $g(t-t')$ and $e^{-\lambda(t-t')}dt$ are functions of the idealised age, which is, the time difference between infiltration and output time. The equation for the mean age of the groundwater sample (τ) is:

$$\tau_s = \int_{-\infty}^{t} (t-t') g(t-t') dt \quad (2)$$

In this study, TracerLPM software (Jurgens et al., 2012) was used for the model calculations. Flow model calculations were conducted using the piston-flow model (PFM), exponential mixing model (EMM), partial exponential model (PEM), and dispersion model (DM) (Maloszewski & Zuber, 2000). The PFM can be applied to hydrogeologic settings where the flow lines are assumed to have

the same residence time, and dispersion and diffusion are negligible. In the EMM approximation, the flow lines are assumed to have an exponential distribution with regard to the residence time. It is applicable to - unconfined aquifers of constant thickness, receiving uniform recharge. The PEM is applicable to the same types of aquifers as for the EMM; however, it is used when only the lower part of the aquifer is sampled. The DM includes dispersion and advective flow, and can give an approximate description of age distributions in samples from many aquifer types. It uses the dispersion parameter (DP), which is the inverse of the Peclet number (Maloszewski and Zuber, 1982, 2002) or the ratio of the dispersion coefficient (D) to the product of velocity (v) and outlet position (x) (Jurgens et al., 2012).

3.5.Agricultural N pressure and comparison with nitrate concentrations in groundwater

One of the primary sources of nitrogen, and simultaneously an indicator of the intensity of agriculture in Croatia, is the fertiliser application per unit area (Romić et al., 2014). The production of mineral fertilisers, demand and prices of agricultural products, and other specific global circumstances influenced the increase in the use of plant nutrients through fertilisation, especially after the Second World War. In Croatia as well in some other EU Member States (e.g., Germany), mineral fertiliser sales statistics are available at the national level (Ondrašek et al., 2021). A fertiliser factory Petrokemija d.d., established in 1968, is a major source of historical data on fertiliser application. As for manure, poultry farms are the primary source in the study area. This study uses available historical data on the production and fertiliser application and manure in both Europe and Croatia. The sources of data were expert reports (Romić et al., 2014), published papers (van Grinsven et al., 2015; Dalgaard et al., 2014; Hansen et al., 2011, 2012, 2017), and statistical data available at Food and Agriculture Organization (FAO) (http://www.fao.org/faostat/en/#data/EF), and Croatian Bureau of Statistics (CBS) (https://www.dzs.hr/hrv/system/stat_databases.htm).

The methodology of comparing nitrate concentrations in groundwater with agricultural N pressures involved several steps. Firstly, collected historical data on nitrate concentrations at each site were

reduced to the mean annual concentrations. Then, the sampling year was converted to the groundwater recharge year assuming a constant groundwater age at each groundwater sampling point (Hansen et al., 2017). This means that the recharge year (i.e. the year when nitrates entered groundwater) was calculated for each annual nitrate concentration as the difference between the sampling year (i.e. the year with the known nitrate concentration at the considered location) and the groundwater age. Finally, the obtained recharge years with the corresponding nitrate concentrations in the groundwater were compared with the historical data of agricultural N pressures.

3.6. Numerical model of groundwater flow and nitrate transport in saturated zone

The evolution of nitrate concentrations in the saturated zone of the aquifer was simulated using a mathematical model. The governing equations for groundwater flow (5) and solute transport (6) were solved numerically using the finite-difference method.

The three-dimensional transient movement of groundwater of constant density through a porous material is described as (Krešić, 2007):

$$\frac{\partial}{\partial x}\left(K_{xx}\frac{\partial h}{\partial x}\right)+\frac{\partial}{\partial y}\left(K_{yy}\frac{\partial h}{\partial y}\right)+\frac{\partial}{\partial z}\left(K_{zz}\frac{\partial h}{\partial z}\right)-W=S_s\frac{\partial h}{\partial t} \quad (3)$$

where K_{xx}, K_{yy}, and K_{zz} are the hydraulic conductivities along the x-, y-, and z- axes (LT^{-1}), which are assumed to be parallel to the major axes of hydraulic conductivity, h is the hydraulic head (L), W is the volumetric flux per unit volume representing sources and sinks (T^{-1}), S_s is the specific storage of the porous media (L^{-1}), and t is time (T).

In general, S_s, K_{xx}, K_{yy}, and K_{zz} are functions of space, and q is a function of space and time. Equation 5 describes the groundwater flow under non-equilibrium conditions in a heterogeneous and anisotropic medium. In the steady-state model, $\frac{\partial h}{\partial t}$ in the governing equation (5) is zero, and the computed heads and fluxes are constant over time.

General equation of solute transport without chemical reactions in three dimensions is (Zheng

&Wang, 1999):

$$\frac{\partial(nC^k)}{\partial t} = \frac{\partial}{\partial x_i}\left(nD_{ij}\frac{\partial C^k}{\partial x_j}\right) - \frac{\partial}{\partial x_{i,j}}(nv_iC^k) + q_sC_s^k \quad (4)$$

where C^k is the dissolved concentration of the species (ML^{-3}), n is the porosity (dimensionless), t is time (T), $x_{i,j}$ is the distance along the respective Cartesian coordinate axis (L), Dij is the hydrodynamic dispersion tensor, v_i is the seepage or linear pore water velocity, calculated as $v_i = {q_i}/{n}$, q_i is the volumetric flow rate per unit volume of aquifer representing fluid sources (positive) and sinks (negative) (T^{-1}), and C_s^k is the concentration of the source or sink flux for species k (ML^{-3}).

A regional three-dimensional numerical groundwater flow model, spanning 2400 km^2 and originally developed in the scope of the research activities focused on groundwater balance in the western and central Drava Valley, was used to assess nitrate concentration evolution in the study area (Fig. 3). The model was set up within the Groundwater Modelling System platform and simulated using the MODFLOW 2005 code (Harbaugh et al., 2017). Horizontal discretisation of the model domain was performed using a grid size of 500 m × 500 m. A vertical discretisation was obtained based on four layers representing the covering aquitard, upper aquifer, aquitard, and lower aquifer. Rivers, accumulation lakes, and drains were implemented into the model as head-dependent boundaries, whereas distributed aquifer recharge, groundwater abstraction at pumping sites, no-flow boundary across the bottom of the modelling domain, and the eastern, western, and southern boundaries were all modelled as specified flux boundaries. Model parameters were initially assigned according to the results of pumping tests carried out mostly for the purpose of the pumping site development and were subsequently adjusted during the calibration process (Table S1).

The model was calibrated in a steady-state with the observed groundwater heads obtained from the network of observation wells (Fig. 4). For calibration purposes, a parameter estimation tool, PEST, was used (Doherty, 2015). In accordance with the parsimony principle (Hill, 2006), the model was kept as simple as possible, and complexity was added in the process of calibration when required. The goodness of fit between simulated and observed heads was evaluated using mean absolute residual (MAR), root mean squared residual (RMS) and normalised root mean squared residual

(NRMS).

Fig. 4.

A three-dimensional numerical model of nitrate transport in the saturated zone of the aquifer was established for the western and central parts of the Drava River Valley, where oxic conditions prevail in the aquifer (Fig. 3). Downstream, the hydrochemical conditions change to anoxic environment, as result of sedimentation, gradually becoming dominant and leading to denitrification processes, which were outside the scope of this study. The model was simulated using the MT3D-USGS code (Bedekar et al., 2016), which is an upgrade to the groundwater flow solution from the MODFLOW code and has the capability to route solutes through dry cells that may occur in the Newton–Raphson formulation of MODFLOW (Niswonger et al., 2011) applied in groundwater flow simulation. The simulation does not consider processes that affect the retardation and decomposition of nitrate, but only the advection-dispersion transport, which is in line with the prevailing hydrochemical conditions of the modelling domain.

Quantification of the three-dimensional dispersion effects on solute transport requires the definition of dispersivity, which is scale-dependent (Wiedemeier et al., 1998; Aziz et al., 2000) and can be determined using laboratory methods, inverse modelling, or empirical expressions. Gjetvaj (1990) investigated the dispersivity in the catchment area of the Varaždin pumping site by monitoring the migration of NaCl solution in a radial flow toward the well. Considering the results of that study, which fall within the range of dispersivities recorded on such a scale (Gehlar at al., 1992), the longitudinal dispersivity of 100, transverse dispersivity of 10, and vertical dispersivity of 1, were used for nitrate transport modelling.

Nitrate inputs were simulated using the Neumann boundary condition for zero inflow rate, and the Cauchy boundary condition for nitrate fluxes at the boundaries with watercourses and lakes, and from agricultural land.

Initial concentrations of nitrate in groundwater in 2006 were derived from national groundwater

quality monitoring datasets. Using linear interpolation method the nitrate concentration values were then interpolated and extrapolated in the areas without information about groundwater quality.

Assessing the accurate fertilisers consumption is a critical point in N balancing, and the most sensitive factor in estimating regional (i.e., at municipality/county level) N surplus (Ondrašek et al., 2021). There are no data on nitrate concentrations in the unsaturated zone of the aquifer in the study area. In the neighbouring Slovenia, Urbanc et al. (2014) determined the nitrate leaching to groundwater from different agricultural lands (uncultivated land and forest, non-intensive land use, extensive land use, intensive land use and nitrate on farmland in Table 3) in the Drava river aquifer system. Both research areas, Croatian and Slovenian, belong to the same river basin and have similar regional hydrogeological characteristics. In addition, there are no significant differences in the agricultural practices of the neighbouring countries regarding the application of fertilizers and manure. Hence, the results of research in Slovenia were used to estimate the nitrate surplus reaching the groundwater from different agricultural lands in the study area. According to Romić et al. (2014), the agricultural land in the modelled area includes the following crops: cereals, corn, sugar beet, soybeans, oilseeds, potatoes, vineyards, meadows, pastures, sunflower, tobacco, vegetables, cabbage, orchards and mosaics. Mosaics were used to represent zones where various crops occupy small areas. In the study area, mosaics occupy around 30%, corn 18%, cereals 7%, vegetables (including potatoes and cabbage) 3.5%, meadows and pastures 8%, and all other crops less than 1% of the total area, with some of them not present at all. For the purpose of this study, different crops listed by Romić et al. (2014) were merged into five agricultural land use classes, based on similar amounts of nitrate leaching according to Urbanc et al. (2014). In total, five classes were identified with nitrate leaching ranging from 7.8 to 81.3 mg/L NO_3 (Fig. 5; Table 3). A particular class was created to account for the increased application of manure to agricultural land in the vicinity of numerous farms. Manure accumulated over time in farm premises is subsequently spread on agricultural land, and the nearest plots are most often used for this purpose (Romić et al., 2014).

Fig. 5.

382 Table 3

383 The transport simulation was performed for a 15-y period from 2006 to 2021, over which a constant
384 input from the sources of nitrates in groundwater was assumed. The simulation results were used to
385 validate the model performance and analyse trends of nitrate concentrations.

386

387 ## 4. Results and discussion

388 ### *4.1.Hydrochemical features and groundwater quality*

389 Groundwater is of the CaMg-HCO_3 hydrochemical type (Larva et al., 2010). This is the primary water
390 type which is principally derived from the dissolution of carbonate minerals (calcite and dolomite)
391 that compose the aquifer. The pH of the groundwater ranges from 7 to 7.5. The electroconductivity
392 (EC) varies from 380 to 790 μS/cm and depends on the amount of dissolved solids in water. Higher
393 EC values are recorded in the shallower parts of the aquifer system.

394 The average oxygen concentrations in groundwater in the upper and lower aquifer are > 3 mg/L, iron
395 concentrations are < 100 μg/L, and nitrates are > 10 mg/L. Because CFCs may be degraded under
396 anoxic conditions, it is important that the study of groundwater age using these tracers is conducted
397 in oxic groundwater.

398 The primary indicator of poor groundwater quality is the high concentration of nitrate. The monitoring
399 of nitrate concentrations has been ongoing for many years, and the historically measured data are
400 presented in Figures 6 and 7. Figure 6a shows the nitrate concentrations from the pumping wells
401 (label B), capturing the upper aquifer; additionally, Figure 6b shows the nitrate concentrations from
402 the observation wells (label P) that also monitor the upper aquifer. Due to high nitrate concentrations,
403 groundwater abstraction from the upper aquifer at the Varaždin pumping site was terminated in the
404 early 2000s. Since then, the nitrate concentrations have been monitored only in the observation wells
405 PDS-5, PDS-6, and PDS-7 (Fig. 6c). In a meantime, the lower aquifer was captured, and nitrate
406 concentrations were monitored in the pumping well B-11 (Fig. 6d). At the Bartolovec pumping site,

407 nitrate concentrations in groundwater were initially measured only in a composite sample (mixture in
408 Figure 7a) that contained groundwater from wells B-1 and B-2 (upper aquifer). Since 2000,
409 measurements have been carried out for each pumping well separately (Figs. 7a and 7b).

410 The highest concentrations of nitrate in groundwater, approximately 140 mg/L in the upper aquifer
411 in the area of the Varaždin and Bartolovec pumping sites, were observed in the early 1980s during
412 the construction of the hydroelectric power plant on the Drava River. Grđan et al. (1991) associated
413 this rise in nitrate concentrations with the filling of the accumulation lake, rise of groundwater levels
414 in the hinterland; these anthropogenic activities, consequently resulted in the leaching of the
415 unsaturated zone.

416 After this period, nitrate concentrations at the Varaždin pumping site remained relatively high,
417 reaching a peak in the mid-1990s (Figs 6 a, b, and c). However, at the Bartolovec pumping site, nitrate
418 concentrations in groundwater in the upper aquifer gradually decreased (Fig. 7a), and subsequently
419 began to rise in the pumping wells B-1, B-2, and B-7 after 2010; however, the same was not observed
420 in the observation boreholes P-2G and P-3G (Fig. 7a). Urumović et al. (1991) suggested that the
421 initial decrease in nitrate concentrations, visible on the composite sample at the Bartolovec pumping
422 site, is a consequence of changes in boundary conditions after the construction of the hydroelectric
423 power plant and the filling of the accumulation lake. Groundwater recharge from the accumulation
424 lake led to a decrease in nitrate concentrations at the Bartolovec pumping site. Water from the Drava
425 River and the accumulation lake does not contain increased nitrate concentrations; hence, the inflow
426 of nitrate-free water into the aquifer results in lower nitrate concentrations in the groundwater.
427 Depending on the trajectories of water particles, this impact is very pronounced in some locations
428 (shallow, 8-m-deep observation wells P-2G and P-3G), but not in others (pumping wells B-1, B-2, B-
429 7).

430 Fig. 6.

431 Nitrate concentrations in the lower aquifer at the Varaždin pumping site have exhibited an increasing
432 trend since initial monitoring in 2002 (Fig. 6d). At the Bartolovec pumping site, the nitrate

concentrations in the lower aquifer have been measured since 1993 and are less than 20 mg/L (Fig. 7b and 7c). In some pumping wells, a slight increase in nitrate concentration has been recorded since 2012 (Fig. 7b).

Fig. 7.

4.2. Interpretation of the mean residence times (MRTs) using environmental tracers

The measured concentrations of CFCs, SF_6 (without correction for excess air), ^3H, and noble gases are given in Table 4. The measured values in pmol/L range from 0.42 to 4.1 for CFC-12, from 0.8 to 30 for CFC-11, and from 0.04 to 0.46 for CFC-113. Samples from boreholes PDS-4, PDS-5, PDS-6, PDS-7, and P-3D show concentrations of CFC-11 and CFC-12 above the equilibrium value (that is, CFC excess). These values are shown in bold in Tables 4. Excess CFC values are usually found in urban areas where there are many pressures on groundwater. The piezometers used for analyses are located in relatively urbanized area, so CFC excess in the shallow part of the aquifer could have been expected. In the case of excess CFCs, groundwater dating is not possible. The measured SF_6 concentrations varied from 1.3 fmol/L in the deep part of the aquifer system to 3.3 fmol/L in the shallow part of the aquifer system.

Table 4

Relating the EAC values to the CFC and SF_6 concentrations in the air in the Northern Hemisphere (https://water.usgs.gov/lab/software/air_curve/index.html), the recharge timing was obtained (Fig. S1).

The measured ^3H concentrations in the groundwater samples ranged from 1.63 to 5.05 TU (Table 4). The measured concentrations of the noble gases were expressed in ccSTP/g (cubic centimetres at an STP dissolved in 1 g liquid water) (Table S2). The sample from the monitoring well BVP-3D is the only sample that is, based on the ^3H content (1.63 ± 0.06 TU) and according to the classification

457 suggested by Clark and Fritz (1997), classified as a mix of sub-modern and modern waters. In other
458 samples, ^{3}H content is 4-5 TU, which classifies them as modern waters.

459 Groundwater ages using the $^{3}H/^{3}He$ method were compared with ^{3}H input data at GNIP stations in
460 Vienna, Ljubljana, and Zagreb (Fig. S2). The GNIP station in Vienna has the longest set of input data.
461 In the period of existence of ^{3}H data at all three stations, the set of Vienna data fits well with the data
462 of the other two stations. Given the proximity of all three stations this is not unexpected. Therefore,
463 the input data from the Vienna station were used for further analyses. The $^{3}H+^{3}He_{(trit)}$ values of all
464 analysed samples match well with the input values of the ^{3}H Vienna station. The groundwater age
465 increases with the sampling depth (Fig. S2).

466 However, some of the groundwater samples display discrepancies between groundwater ages
467 estimated by different tracers. The groundwater ages of samples PDS-5, PDS-6, and PDS-7 using
468 CFC-113 suggest greater ages compared to that estimated from the SF_6 and $^{3}H/^{3}He$ methods.
469 Concentrations of CFC-11 and CFC-12 above the equilibrium value were determined on all three
470 samples. Although the concentration of CFC-113 is not above the equilibrium value, it is still
471 significantly high, which is why it shows older water than the one that, given the hydrogeological
472 conditions of the investigated site, can be. The groundwater ages obtained for the PDS-4 and P-3D
473 samples using CFC-113 and $^{3}H/^{3}He$ were very similar (~30 y). For BVP-3P and BVP-3D samples,
474 groundwater ages determined using all three CFCs and $^{3}H/^{3}He$ were similar (24.2–36 y for BVP-3P,
475 and 50–62.1 y for BVP-3D, respectively). Comparatively, the groundwater ages determined by SF_6
476 are approximately half for the BVP-3D and P-3D samples and 3–5 times less for BVP-3P. Lower SF_6
477 groundwater ages may result from a slight excess of air that could originate from low levels of
478 contamination (Busenberg & Plummer, 2000; Zoellmann et al., 2001, Wilske et al., 2020).
479 MacDonald et al. (2003) found that due to the lower solubility, SF_6 concentrations were less buffered
480 against changes due to unintentional air entry during sampling. Accordingly, it could be concluded
481 that there was either an unintentional air entry during sampling or that the groundwater sample

contained excess SF_6 that could have originated from a low level of pollution. Because the bottles of the samples did not contain bubbles, the second option is deemed more likely.

The consistency of the groundwater ages was verified based on the assumption that the vertical velocity v_{vert} at the water table surface is simply a function of the recharge rate R and the porosity p according to the relation $v = R/p$ (Mahlknecht et al., 2001). The travel time t for vertical movement from the water table to sampling depth d is $t = d/ v_{vert} = d\ x\ (p/R)$. The travel time for groundwater samples was calculated for the recharge rates from 20% to 30% of the mean annual precipitation and porosity of 0.23 (Table 5).

Table 5

The resulting groundwater ages generally increase with depth and are quite consistent, according to most methods. In all cases, mixing and dispersion were neglected, that is, piston-flow conditions were assumed. The influence of mixing and dispersion on MRT was analysed using LPMs (Figs. S3-S5).

Graphical estimation of the mean groundwater age of the samples PDS-5 and PDS-6 from a shallow part of the aquifer system is displayed in Fig. S3. The results of the PFM fit well with the measured tracers ^3H and $^3H_0$. All models are consistent with the $^3He_{(trit)}$ and $^3H/^3H_0$ values of the sample. The DM is consistent with the SF_6 and $^3H/^3H_0$ values of the sample PDS-5 and a DP of 1. The EMM is consistent with the SF_6 and $^3H/^3H_0$ values of the sample PDS-6. The PFM, PEM, and EMM are consistent with the SF_6 and $^3He_{(trit)}$ values of both samples. For all models, the mean groundwater ages of the samples are < 10 y.

Graphical estimation of the mean groundwater age of the samples P-3D and BVP-3P is presented in Fig. S4. A deeper part of the upper aquifer was tapped by these observation wells. The PEM results agree with the measured tracers ^3H and ^3Ho as well as the $^3He_{(trit)}$ and $^3H/^3H_0$ in the sample P-3D. It yielded an optimised mean age of 25 y with a PEM ratio of 0.1. The EMM and DM models are consistent with the SF_6 and $^3He_{(trit)}$ values of the sample. The MRT is ~20 y. The CFC-113 and $^3H/^3H_0$ values of the sample P-3D are the nearest to the PFM model results and the MRT corresponds to ~32 y.

In the groundwater sample BVP-3P, the PFM agrees well with the measured tracers ^{3}H and $^{3}H_0$ as well as the $^{3}He_{(trit)}$ and $^{3}H/^{3}H_0$. The mean groundwater age is estimated to be ~25 y. The DM models with a DP of 1 are consistent with the SF_6 and $^{3}He_{(trit)}$ values of this sample. However, the models yield an optimised mean age of ~10 y. The CFC-113 and $^{3}H/^{3}H_0$ values do not fit with any of the models. The PFM agrees well with the measured tracers CFC-12 and CFC-113, and the estimated mean groundwater age is ~35 y.

Graphical estimation of the mean groundwater age of the samples PDS-4 and BVP-3D is presented in Fig. S5. These observation wells tap the lower aquifer. For the ^{3}H and $^{3}H_0$ methods, as well as for the SF_6 and $^{3}He_{(trit)}$, the measured tracers of PDS-4 are located between the PFM and the PEM model. The mean groundwater age is ~25 y. For the $^{3}He_{(trit)}$ and $^{3}H/^{3}H_0$ the measured tracer in the sample PDS-4 is located closer to the PEM than the PFM model with the MRT of ~25 y. The PFM is consistent with the CFC-113 and $^{3}H/^{3}H_0$ values of the sample and the MRT corresponds to 30 y. The DM yields an optimised mean age of 70 y with DP of 1 (for CFC-12 and CFC-113). The PFM results of the groundwater sample BVP-3D agrees well with the measured tracers ^{3}H and $^{3}H_0$, as well as the $^{3}He_{(trit)}$ and $^{3}H/^{3}H_0$. The mean groundwater age is ~70 y. The DM with a DP of 1 is consistent with the SF_6 and $^{3}He_{(trit)}$ values of this sample and gives the mean groundwater age of ~60 y. For the CFC-11 and $^{3}H/^{3}H_0$ methods, the measured tracer in the sample BVP-3D is located closer to the PFM model with the MRT of ~80 y. The CFC-113 and $^{3}H/^{3}H_0$ values of this sample do not correlate with any models. Graphical estimation of the mean groundwater age of the sample BVP-2D does not return any reliable results.

A more accurate determination of the mean groundwater age was found using a calculation of the best-fit mean age (Table 6). The best-fit mean age is consistent with the applicability of individual models to specific groundwater flow from a recharge area to a measured position in the observation wells. Observation wells PDS-5 and PDS-6 tap relatively thin, unconfined aquifers of approximately uniform thickness in the recharge area, receiving uniform recharge, and accordingly, the best-fit mean ages are given by EMM and DM. In contrast, the samples PDS-4, BVP-2D, BVP-3P, and BVP-3D

were collected from greater aquifer depths and their best-fit mean ages are, therefore, given by PEM and DM.

Table 6

4.3.Vertical age profiles

Vertical profiles of tracer values in an aquifer system are among the most valuable data for understanding the flow system (IAEA, 2013). The resulting CFCs, SF_6, and $^3H/^3He$ ages generally increase with depth, ranging from ~8 y in the upper aquifer to > 50 y in the lower aquifer. In the deeper part of the upper aquifer, the MRT was estimated to be ~29 y (mean MRT values for BVP-3P in Table 6). A downward vertical groundwater velocity ranges from ~0.75 to 2 m/year, as estimated by dividing the depth of the screen by the $^3H/^3He$ ages of the samples, ignoring the dispersion (Table 5).

The covering aquitard above the aquifer is made of clay, silt, and sand, and its thickness ranges from 0 to 2 m. The thickness of these deposits increases toward the southern boundary of the Drava River Valley. The thickness of the unsaturated zone in the study area ranges from 2 to 6 m. According to research conducted in similar hydrogeological conditions upstream of the study area, in Slovenia, it was found that the mean flow velocity through the unsaturated zone approximately ranges from 0.01 to 0.026 m/day (Koroša et al., 2020). In accordance with the thickness of the unsaturated zone, the total travel time through the unsaturated zone lasts between 0.2 and 1.6 y. Considering the relatively short duration of the flow through the unsaturated zone, it can be concluded that its addition does not significantly increase the groundwater age and is practically within the error of the estimated age of water using a tracer.

4.4.Groundwater age distributions

Groundwater age distributions in the selected samples PDS-5 (the shallowest part, upper aquifer), BVP-3P (deeper part of the upper aquifer), and BVP-3D (the lower aquifer) were analysed and are shown in Figures 8, 9, and 10. The age distribution displays the fractional contribution of each sub-parcel of water that collectively constitute the entire sample (Jurgens et al., 2012). The EMM and DM yield similar age distributions in the sample PDS-5, and both indicate that water contributing to the well has a distribution of ages from a few to 70 y (Fig. 8a). The models indicate that the amount of young water (~8 y) reaching the well is 80% for the DM and 70% for the EMM, and only ~20% of the water from this well is > 10 y (Fig. 8b).

Fig. 8.

The PEM and DM yield similar age distributions for the sample BVP-3P. Both models indicate that water samples show a distribution of ages from a few to ~43 y for the PEM, and several times more for the DM (Fig. 9a). The amount of water < 30 y was ~75% for all models, and < 10% of the water in this sample was > 100 y according to the DM (Fig. 9b).

Fig. 9.

The PEM and DM indicate that water contributing to BVP-3D shows a distribution of ages from a few years for the DM or ~20 y for the PEM, to > 500 y for the DM and ~150–180 y for the PEM (Fig. 10a). The amount of water younger than 50 y reaching the well was ~ 60% for the DM, and ~30% for the PEM. Approximately 20% of the water in this sample was older than 100 y for the DM, and ~ 50% for the PEM (Fig. 10b).

Fig. 10.

4.5.Agricultural N pressures on groundwater and relationship with nitrate concentration trend

The significant use of mineral fertilisers in Croatia began in the 1960s (Romić et al., 2014). According to Petrokemija d.d., the consumption of mineral fertilizers since 1995 has varied from 400 to 450 thousand tons per year, which is significantly less than the consumption before 1990 (Fig. 11a).

583 According to the FAO database, these amounts are even lower, but the trend is reversed. This
584 difference is probably due to the fact that Petrokemija shows the amount of fertiliser sold while the
585 FAO statistics relies on the consumed fertiliser amounts. Nevertheless, the use of mineral nitrogen
586 fertilisers in Croatia in the period 2012–2015 was decreased by 30% compared to 2008–2011 (EC,
587 2018).

588 Fig. 11.

589 The fertilizer application curve for the EU is similar to the curve of historical fertiliser application
590 according to Petrokemija (Fig. 11a). In both curves, it is clear that in the late 1980s, there was a
591 relatively sharp decline in fertiliser application. A similar distribution of fertiliser use has also been
592 observed in Denmark (Hansen et al., 2010, 2012, 2017). Van Grisven et al. (2015) state that there are
593 several reasons for the reduction in fertiliser application in the EU. First, after the collapse of the
594 Soviet Union in 1991, the transition of a centrally planned system of large collective state farms to a
595 market-based system in Eastern European countries ceased the subsidies for the purchase of
596 fertilisers. Second, MacSharry's 1992 EU reform (the common agricultural policy) reduced
597 commodity support for cereal production and introduced mandatory land provisions in Western
598 European countries, which reduced fertiliser demands (Stouman-Jensen et al., 2011). Third, the
599 European Union imposed strict regulations on N use in agriculture in the 1970s. Furthermore, during
600 the Homeland War in Croatia in the 1991–1995 period, agriculture, like all other industries, was
601 neglected, which resulted in a sharp decline in fertiliser sales and consumption.

602 Van Grinsven et al. (2015) also demonstrated that the time distribution of pressures from mineral
603 fertilisers and manure in the EU countries display a similar trend, which suggests that the pressure
604 from manure from the 1990s has been declining. The data provided by the FAO database indicate
605 similar trends (Fig. 11b). There is no historical data on manure consumption in Croatia, but in
606 accordance with the already described situation, the same trend is expected, as in the rest of the EU.
607 The manure consumption data in Croatia collected for the last decade, do not indicate any pronounced
608 trend of change (Fig. 11a).

There are also no long-term historical data on the N surplus in Croatia. These data have been collected since 2010 and indicate that the N surplus averages at ~65% of the fertiliser application (Fig. 11a). The N surplus generally follows the trend of N input (Fig. 11b). According to research conducted from July 2011 to December 2012 in the Varaždin area, a total N content of 150–700 kg/ha was found in the 1 m soil profile, indicating excessive fertiliser use (Bubalo et al., 2014). A maximum of 32% leached N suggests that there is a direct agricultural influence on groundwater quality.

In accordance with aforementioned, the assessment of nitrate evolution in groundwater was made on the basis that fertiliser application according to Petrokemija reflects the total agricultural pressure in Croatia. In this study of the dependence of historical nitrate concentrations in groundwater (Figs. 6c, 6d and 7c) on the mean values of groundwater age (Table 6), agricultural pressure trends were crucial, and not their absolute amounts.

Considering the MRT of 8 y in the upper aquifer at the catchment area of the Varaždin pumping site, a relatively good agreement of the trends is observed for the historical pressure from agricultural activity and nitrate concentrations in groundwater (Fig. 12). The trends also coincide in the lower aquifer tapped at the Varaždin pumping site for the mean value of groundwater age of 24 y.

Fig. 12.

Grđan et al. (1991) concluded that the abrupt increase in nitrate concentrations in groundwater determined in 1982 could not be related to the application rate of mineral fertiliser applied because the consumption of mineral fertilisers in the Varaždin area began to decrease due to poor market opportunities. The authors corroborate this with the fact that the application rate of mineral fertilisers applied in the early 1980s was lower than that in the 1970s. Despite higher consumption, then the nitrate concentration in groundwater was ~66 mg NO_3/L, and in 1982 was 98 mg NO_3/L (Fig. 4). However, the authors did not consider the MRT. Given the high consumption of mineral fertilisers recorded in the mid-1970s, and the MRT of ~8 y, and with the increase in groundwater levels caused by the filling of the accumulation lake, an increase in nitrate concentration in the early 1980s is not surprise. Trends similar to those in Fig. 11a are also observed on comparing the quantities of applied

635 mineral fertiliser listed in Grđan et al. (1991) with the corresponding nitrate concentrations in the
636 recharge year (Fig. 13).

637 Fig. 13.

638 In the upper aquifer tapped at the Bartolovec pumping site for the mean value of groundwater age of
639 29 y the trends of historical pressure from agricultural activity from early 70s and nitrate
640 concentrations in groundwater display relatively good agreement (Fig. 14). The high nitrate
641 concentration in groundwater registered in the early 1980s (Fig. 7a) cannot be related to the
642 agricultural pressure curve in Fig. 14. At that time, only shallow pumping wells B-1 and B-2 were in
643 operation. The sudden increase in groundwater levels is caused by the filling of the accumulation
644 lake. Shallow water table make nitrate entering groundwater more easily and consequently
645 determined the nitrate loading from vadose zone (Guo et al., 2006). Subsequent changes of the
646 boundary conditions and the catchment area of the Bartolovec pumping site, and the inflow of nitrate-
647 free water, allowed decreasing of the nitrate concentration. However, with a dominant groundwater
648 inflow of the MRT of 29 years from more remote, primarily western areas of the catchment, the nitrate
649 concentration in groundwater began to increase again, which corresponds to the considered
650 agricultural pressure (Fig 14).

651 Fig. 14.

652 The results of the assessment of nitrate evolution are supported by the results of the groundwater age
653 distribution of in the aquifer system. Groundwater in the shallowest part of the system contains
654 approximately 80% of water younger than 8 years (Fig. 8), and the mean annual concentration of
655 nitrate in the water reached 100 mg/L (Fig. 12). In the deeper part of the upper aquifer (Bartolovec
656 pumping site), groundwater contains approximately 75% of water younger than 30 years (Fig. 9), and
657 the mean annual concentration of nitrate in the water reached 30 mg/L (Fig. 14). In the lower aquifer,
658 the groundwater age is determined to be approximately 24 years (Varaždin pumping site) and more
659 than 50 years (Bartolovec pumping site). The aquitard separating the upper and lower aquifers is not
660 continuous in the Varaždin area (Fig. 2), and consequently, the concentration of nitrate in

661 groundwater reached 60 mg/L. At the Bartolovec pumping site, groundwater in the lower aquifer
662 contains up to 60% of water younger than 50 years (Fig. 10), and nitrate concentrations reach 15
663 mg/L (Fig. 7c). According to the applied methodology, the increase in nitrate concentrations in this
664 aquifer can last for years.

665 This study demonstrates a clear relationship between changes in agricultural pressure, and change in
666 the nitrate concentrations with the similar temporal pattern and trend reversals. These findings are
667 comparable with previous studies conducted in Denmark (Hansen et al., 2011; 2012) and the
668 Netherlands (Broers & van der Grift, 2004; Visser et al., 2009). The nitrate concentrations in the
669 Denmark were decreased after recharge year 1980, and in the Netherlands, as well as in Croatia,
670 decreasing of the nitrate concentration began approximately 10 years later (around 1990). The
671 recharge years were defined on the same way. The difference is in the applied agricultural N pressure.
672 Hansen et al. (2012) has applied N surplus which is considered to be the best indicator of the impact
673 of agriculture on the environment in a given period (European Environmental Agency, 2005) and
674 which represents the amount of N deposited in the soil that is not used in production system (plants
675 do not absorb all fertilizers), which is why the environment is endangered (Dalgaard et al., 2011;
676 Hansen et al., 2012). Unfortunately, there are no historical data on N surplus in Croatia. As
677 aforementioned, in this study the nitrate concentration trend was compared with the trends of
678 application of mineral fertilizers and manure. Given that the curve of historical data of the N surplus
679 generally has the same trend as the total agricultural pressure (Fig. 11), this approach can be
680 considered acceptable both in this case study and in all other locations where there is no historical
681 data of the N surplus, but there is data on total pressure.

682

683 *4.6. Numerical simulation of the nitrate concentrations evolution in the aquifer system*

684 The model performance was evaluated using the calibration error statistics (Fig. S6). According to
685 calibration results (MAR = 0.70 m, RMS= 0.83 m, NRMS = 0.90%), the model performs reasonably
686 well and forms a solid basis for a solute transport simulation. The validation of the solute transport

687 model was performed by comparing the simulated and observed nitrate concentrations. The evolution
688 of nitrate concentration in the shallow aquifer in the catchment area of the former Varaždin pumping
689 site for the period from 2006 to 2021 is shown in Figures 15. This area is characterised by the highest
690 initial nitrate concentrations in the study area. The simulated values correspond well with
691 observations, especially for the wells PDS-5 and PDS-6. For the observation well PDS-7, the
692 simulated values are altogether overestimated, most probably because of the overestimated initial
693 nitrate concentrations in the vicinity of the well. However, the direction of the simulated curve follows
694 the direction of the observed concentrations reasonably well. The simulation curves for all wells
695 indicate a slight declining trend in nitrate concentration towards the end of the simulation, which is
696 generally in line with the conclusions drawn from the mean groundwater age estimates and historical
697 agriculture pressure (Fig. 12).

698 Fig. 15.

699 The aquifer system is thicker in the catchment area of the Bartolovec pumping site, compared to the
700 Varaždin pumping site. Consequently, vertical stratification in terms of both mean groundwater age
701 and groundwater quality is more pronounced. The effects of local influences (groundwater
702 abstraction, seepage from accumulation lake, drains, application of fertilisers, and manure) and the
703 effects of regional flow, are also reflected in the distribution of nitrate concentrations in the pumping
704 site and its catchment area, as shown in Figure 5. Thus, the observation wells P-2G and P-3G that tap
705 shallow parts of the upper aquifer with relatively young groundwater exhibit low nitrate
706 concentrations. In contrast, groundwater samples from the pumping wells, which are representative
707 of regional groundwater flow, have distinctly higher nitrate concentrations, even though there are
708 differences in nitrate concentrations between individual wells as a consequence of the geometry of
709 their catchment areas.

710 Vertical and horizontal discretisation of the regional three-dimensional numerical model does not
711 allow for a detailed analysis of the local influences on groundwater flow and nitrate concentration
712 distribution. In this regard, and in accordance with the aforementioned, observed nitrate

concentrations from the pumping wells, which are representative of regional groundwater flow in the upper and lower aquifers, were used to evaluate the model performance (Fig. 16). The simulated curve represents the evolution of nitrate concentrations at the abstraction site and is plotted against nitrate concentrations in individual wells (Fig. 16). It can be seen that the model is unable to reproduce variations in concentrations over simulation time, primarily because we assumed steady-state conditions for both groundwater flow and nitrate transport model. However, the simulated values correspond with the general trend in both the upper and lower aquifers. Both simulation curves indicate a positive trend of nitrate concentrations towards the end of the simulation, which is consistent with the trends of observed nitrate concentrations.

Fig. 16.

The aim of this study was to improve the understanding of temporal changes in nitrate concentration in groundwater and to investigate the association of nitrate in groundwater with agricultural load. In the presented approach, the groundwater age dating and historical agricultural pressure data, together with the results of nitrate transport modelling, were used to interpret the nitrate trends (Fig. 3). This is the first time that an assessment of the groundwater age was made in the study area, and the findings were supported by the results of three-dimensional numerical model of nitrate transport through the saturated zone of aquifer. The results obtained in the study demonstrate that, even in the areas lacking detailed temporal data on agricultural pressures, the applied methodological approach yields valuable results that help explain the evolution of nitrate in aquifer system. Groundwater age dating was once again proved to be an important indicator of the groundwater vulnerability and, together with the modelling of groundwater flow and solute transport should be an integral part of decision-making process in the frame of the sustainable groundwater management. The integrated methodological approach applied can help assess the effectiveness of protection measures and the implementation of the EU Water Framework Directive and Nitrate Directive.

5. Conclusion

739 This study demonstrates that groundwater age provides valuable information for groundwater
740 management. A relationship was observed between fertiliser application in agriculture and nitrate
741 concentrations in groundwater with similar temporal trends. Spatial groundwater age causes
742 variations in the concentration of nitrates. The MRT of groundwater is < 10 y in the shallow part of
743 the aquifer, ~30 y at the monitoring depth of 35 m, and > 50 y in the monitored part of lower aquifer.
744 Groundwater age distribution in the groundwater samples indicated that the proportion of young
745 groundwater decreased in the vertical section of the aquifer system. Approximately 80% of the
746 groundwater at typical monitoring depths of ~15 m was younger than 10 y. At a monitoring depth of
747 35 m, ~75% of the groundwater was younger than 30 y. In the monitored part of lower aquifer, up to
748 60% of the groundwater was younger than 50 y.

749 The decrease in fertiliser application caused a decrease in the nitrate concentrations in the youngest
750 oxic groundwater. However, the trend of increasing nitrate concentrations at the deepest monitoring
751 site of the aquifer can last for years.

752 The spatiotemporal development of nitrate concentrations in groundwater, simulated by a three-
753 dimensional numerical model, is consistent with the observations. The results indicate a negative
754 trend of nitrate concentrations in the shallow aquifer system with young groundwater, and the same
755 trend is expected in the future based on the simulation curve. This is consistent with the trend of
756 historic values and conclusions inferred from the mean groundwater age assessment and fertiliser
757 application relationship. Owing to a coarse grid, in a complex aquifer system the model was unable
758 to simulate the horizontal and vertical distribution of nitrate concentrations in detail. However, the
759 simulated curve fits the observations reasonably well and captures the trend of historic values. Future
760 studies can focus on developing a local numerical model with finer vertical and horizontal
761 discretisation that will provide a comprehensive comparison of groundwater age distributions derived
762 from the groundwater flow model with advective particle tracking and environmental tracer analysis,
763 and facilitate the simulation of future evolution of nitrates in the aquifer system.

764 This study highlights the importance of understanding groundwater age in water resource
765 management. The implementation of the EU WFD and Nitrate Directive, among several other
766 directives, often requires various protection measures. However, for effective evaluation of the
767 implemented measures, it is crucial to keep in mind that the time required for the effects of these
768 measures to take place depends on the groundwater age and its distribution.

769

770 **Acknowledgments**

771 This paper was made as a part of the GeoERA HOVER project, which is supported by the EU Horizon
772 2020 research and innovation program [grant agreement No. 731166]. It is also partly the result of
773 training and education conducted through GeoTwinn project that has received funding from the EU
774 Horizon 2020 research and innovation programme under grant agreement No. 809943. The authors
775 wish to express their gratitude to Hrvatske vode which participated in research funding [No. 2804/19].
776 The authors are grateful to Hrvatske vode and Varkom Ltd. for providing groundwater quality data.
777 Special thanks to Dr. Laszlo Palcsu for tritium and noble gas isotope analyses, and the $^{3}H/^{3}He$ age
778 calculation, and Dr. Harald Oster for CFCs and SF_6 analyses. The authors wish to thank reviewers
779 and editors for their very useful comments which have helped improve the manuscript.

780

781 **References**

782 Aziz, C.E., Newell, C.J., Gonzales, J.R., Haas, P., Prabhakar Clement, T. & Yunwei Sun (2000):
783 BIOCHLOR: Natural Attenuation Decision Support System; User's manual, version 1.0. EPA/600/R-
784 00/008, U.S. Environmental Protection Agency, Office of Research and Development, 46 p.,
785 Washington, D.C.

786 Basso, B., Ritchie, J. T. (2005). Impact of compost, manure and inorganic fertilizer on nitrate leaching
787 and yield for a 6-year maize–alfalfa rotation in Michigan. Agriculture, Ecosystems and Environment
788 108, 329-341.

Bedekar, V., Morway, E.D., Langevin, C.D., and Tonkin, M. (2016): MT3D-USGS version 1.0.0: Groundwater Solute Transport Simulator for MODFLOW: U.S. Geological Survey Software Release, 30 September 2016, http://dx.doi.org/10.5066/F75T3HKD

Broers, H. P. & van der Grift, B. (2004): Regional monitoring of temporal changes in groundwater quality. J. Hydrol., 296, 192-220.

Bu, X. & Warner, MJ (1995): Solubilities of chlorofluorocarbons 113 in water and seawater. Deep-Sea Research Part I: Oceanographic Research Papers, 42/7, 1151-1161.

Bubalo. M., Romić, D., Zovko, M. & Kuspilić, N. (2014): Agricultural Impact on Groundwater Vulnerability to Nitrate in Northern Croatia. Agric. Conspec. Sci., 79 (1), 23-29.

Busenberg E. & L.N. Plummer, 2000. Dating young groundwater with sulfur hexafluoride: Natural and anthropogenic sources of sulfur hexafluoride. Water Resour. Res., v. 36, p. 3011-3030, October 2000.

Cambray, A.R., Marks, M.J., Dawes, S., Ward, R., Hallard, M., MacDonald, A.M., Ruddle, O. & McConvey, P. (2005): Monitoring effectiveness of the EU Nitrate Directive Action Programmes: Approach by the United Kingdom. RIVM report.

Chambers, L.A., Gooddy, D.C. & Binley, A.M. (2019): Use and application of CFC-11, CFC-12, CFC113 and SF_6 as environmental tracers of groundwater residence time: A review. Geosci. Front., 10, 1643-1652.

Clark & Fritz (1997): Environmental isotopes in hydrogeology. Lewis Publishers, London, p. 328.

Cook, P.G.& Herczeg, A.L. (1998): Groundwater chemical methods for recharge studies. Csiro Publishing. p. 24.

Cook, P.G.& Herczeg, A.L. (2000): Environmental Tracers in Subsurface Hydrology. Springer, p. 529.

812 Cook, P.G. and Solomon, D.K. (1995). Transport of atmospheric trace gases to the water table:
813 Implications for groundwater with chlorofluorocarbons and dating krypton 85. Water Resour. Res.,
814 31, 263-270.

815 Cosgrove, B.A. & Walkley, J. (1981): Solubilities of gases in H2O and 2H2O. J. Chromatogr. A, 216,
816 161-167.

817 Dalgaard, T., Hutchings, N., Dragosits, U., Olesen, J. E., Kjeldsen, C., Drouet, J.,L., & Cellier, P.
818 (2011): Effects of farm heterogeneity on modelling and upscaling of nitrogen losses and greenhouse
819 gas emissions in agricultural landscapes, Environ. Pollut., 159, 3183–3192.

820 Dalgaard, T., Hansen, B., Hasler, B., Hertel, O., Hutchings, N.J., Jacobsen, B.H., Jensen, L.S.,
821 Kronvang, B., Olesen, J.E., Schjørring, J.K., Kristensen, I.S., Graversgaard, M., Termansen, M. &
822 Vejre, H. (2014): Policies for agricultural nitrogen management—trends, challenges and prospects
823 for improved efficiency in Denmark. Environ. Res. Lett., 9, 115002.

824 Doherty, J. (2015): Calibration and uncertainty analysis for complex environmental models.
825 Watermark Numerical Computing .

826 Dulinski, M.; Rozanski, K.; Pierchala, A.; Gorczyca, Z.; Marzec, M. Isotopic composition of
827 precipitation in Poland: a 44-year record. Acta Geophys. 2019, 67, 1637-1648.

828 EC (2018): Report from the Commission to the Council and the European Parliament on the
829 implementation of Council Directive 91/676/EEC concerning the protection of waters against
830 pollution caused by nitrates from agricultural sources based on Member State reports for the period
831 2012-2015, (COM(2018) 257 final, 4 May 2018), European Commission, Brussels.

832 European Environmental Agency (2005): Agriculture and environment in EU-15 – the IRENA
833 indicator report, EEA Report No 6/2005 ISBN 92-9167-779-5, ISSN 1725-9177, EEA,
834 Copenhagen.

835 Gelhar, L.W., Welty, C. & Rehfeldt, K.R. (1992): A critical review of data on field-scale dispersion
836 in aquifers. Water Resour. Res., 19(1), 161-180.

837 Gjetvaj, G. (1990): Identification of dispersivity parameters in radial flow. Proceedings of the 10th
838 Conference of the Yugoslav Society for Hydraulic Research, 436-440, Sarajevo.

839 Grđan D., Durman, P. & Kovačev-Marinčić, B: (1991): Relationship between regime change and
840 groundwater quality at Varaždin and Bartolovec pumping sites (in Croatian). Geol. vj., 44, 301-308.

841 Guo H., Li, G., Zhang, D., Zhang, X. & Lu. C. (2006): Effects of water table and fertilization
842 management on nitrogen loading to groundwater. Agric. Water Manag., 82, 86–98.

843 Hansen, B., Thorling, L., Dalgaard, T. & Erlandsen, M. (2011): Trend Reversal of Nitrate in Danish
844 Groundwater - a Reflection of Agricultural Practices and Nitrogen Surpluses since 1950. Environ.
845 Sci. Technol., 45(1), 228-34. DOI: 10.1021/es102334u

846 Hansen, B., Dalgaard, T., Thorling, L., Sorensen, B. & Erlandsen, M. (2012): Regional analysis of
847 groundwater nitrate concentrations and trends in Denmark in regard to agricultural influence.
848 Biogeosciences, 9, 3277–3286.

849 Hansen, B., Thorling, L., Schullehner, J., Termansen, M. & Dalgaard, T. (2017): Groundwater nitrate
850 response to sustainable nitrogen management. Sci. Rep., 7:8566. DOI: 10.1038/s41598-017-07147-2

851 Harbaugh, A.W., Langevin, C.D., Hughes, J.D., Niswonger, R.N., and Konikow, L. F. (2017):
852 MODFLOW-2005 version 1.12.00, the U.S. Geological Survey modular groundwater model: U.S.
853 Geological Survey Software Release, 03 February 2017, http://dx.doi.org/10.5066/F7RF5S7G

854 Hill, M.C. (2006): The practical use of simplicity in developing ground water models. Ground Water,
855 44, 775-781.

856 IAEA (2006): Use of chlorofluorocarbons in hydrology, p. 277.

857 IAEA (2013): Isotope Methods for Dating Old Groundwater. p. 357.

858 IAEA/WMO: Global network of isotopes in Precipitation. The GNIP database. Available online at
859 http://www-naweb.iaea.org/napc/ih/IHS_resources_gnip.html

Jurgens, B.C., Böhlke, J.K. & Ebarts, S. (2012): TracerLPM (Version 1): An Excel® Workbook for Interpreting Groundwater Age Distributions from Environmental Tracer Data. U.S. Geological Survey Techniques and Methods Report 4-F3, p. 60.

Kazemi, G., A., Lehr, J.H. & Perrochet, P. (2006): Groundwater Age. John Wiley & Sons, p. 288.

Koroša, A., Brenčič, M. & Mali, N. (2020): Estimating the transport parameters of propyphenazone, caffeine and carbamazepine by means of a tracer experiment in a coarse-gravel unsaturated zone. Water Res., 175: 1-12. doi: 10.1016/j.watres.2020.115680

Kovač, I., Kovačev-Marinčić, B., Novotni-Horčička, N., Mesec, J. & Vugrinec, J. (2017): Comparative analysis of nitrate concentration in upper and lower aquifer of the Varaždin system of aquifers (in Croatian). Radovi Zavoda za znanstveni rad Varaždin, 28/1, 41-57 doi:10.21857/9e31lh4zem

Krajcar Bronić, I., Barešić, J., Borković, D., Sironić, A., Lovrenčić Mikelić, I. & Vreča P. (2020): Long-term isotope records of precipitation in Zagreb, Croatia. Water, 12, 226. doi:10.3390/w12010226

Kreft, A. & Zuber, A. (1978): On the physical meaning of the dispersion equation and its solution for different initial and boundary conditions: Chem. Eng. Sci., 33/11, 1471–1480. Available online at URL http://www.sciencedirect.com/science/article/ pii/0009250978851963

Krešić, N. (2007): Hydrogeology and groundwater modelling. CRC Press, p. 807<.

Larva, O. (2008) Aquifer vulnerability at catchment area of Varaždin pumping sites. PhD thesis (in Croatian), University of Zagreb, p. 198.

Larva, O., Marković, T., Brkić, Ž. (2010): Groundwater hydrochemistry of the Quaternary alluvial aquifer in Varaždin region - Croatia // XXXVIII IAH Congress Groundwater Quality Sustainability Abstract Book / Zuber, A., Kania, J. & Kmiecik, E. (ur.), Krakow, Poland, University of Silesia Press, 135-136.

884 Lindsey, B.D., Philips, S.W., Donnelly, C.A., Speiran, G.K., Plummer, L.N., Bohlke, J.K., Focazio,
885 M.J., Burton, W.C. & Busenberg, E. (2003): Residence times and nitrate transport in ground water
886 discharging to streams in the Chesapeake Bay Watershed. USGS, Water-Resources Investigations
887 Report 03-4035.

888 MacDonald, A.M., Darling, W.G., Ball, D.F. & Oster, H. (2003): Indetifying trends in groundwater
889 quality using residence time indicators: an example from the Permian aquifer of Dumfries, Scotland.
890 Hydrogeol. J, 11, 504-517.

891 Mahlknecht, J., Schneider, J.F. & Oster, H. (2001): CFCs and SF6 in aquifers investigations - The
892 significance of the unsaturated zone and the origin of groundwater. Available online at
893 https://www.semanticscholar.org/paper/CFCs-and-SF6-in-aquifers-investigations-The-of-the-
894 Mahlknecht/dbe32e3f8bf0e21529c3654de4786cc3846be18b#paper-header

895 Maloszewski, P. & Zuber, A. (1982): Determining the turnover time of groundwater systems with the
896 aid of environmental tracers: 1. Models and their applicability. J. Hydrol., 57/3–4, 207–231.

897 Maloszewski, P., Rauert, W., Trimborn, P., Herrmann, A. & Rau, R., (1992): Isotope hydrological
898 study of mean transit times in an alpine basin (Wimbachtal, Germany). J. Hydrol., 140, 343-360.

899 Maloszewski, P., Zuber, A., 1996. Lumped parameter models for interpretation of environmental
900 tracer data. In: IAEA (Ed.), Manual on the mathematical models in isotope hydrogeology.
901 International Atomic Energy Agency, Vienna, pp. 9-59.

902 Maloszewski P., Stichler, W., Zuber, A. & Rank, D. (2002): Identifying the flow systems in a karst-
903 fissured-porous aquifer, the Schneealpe, Austria, by modelling of environmental 18O and 2H
904 isotopes. J. Hydrol., 256 (1-2), 48-59.

905 Modica, E., Buxton, H.T. & Plummer, L.N. (1998): Evaluating the source and residence times of
906 groundwater seepage to streams, New Jersey Coastal Plain. Water Resour. Res., 34, 2797-2810.

907 Niswonger, R.G., Panday, Sorab, and Ibaraki, Motomu (2011): MODFLOW-NWT, A Newton
908 formulation for MODFLOW-2005: U.S. Geological Survey Techniques and Methods 6–A37, 44 p.

909 Ondrašek, G., Bakić Begić, H., Romić, D., Brkić, Ž., Husnjak, S. & Bubalo Kovačić, M. (2021): A
910 novel LUMNAqSoP approach for prioritising groundwater monitoring stations for implementation
911 of the Nitrates Directive. Environ. Sci. Eur. 33, 23.

912 Oster, H., Sonntag, C., & Münnich, K. O. (1996): Groundwater age dating with chlorofluorocarbons.
913 Water Resour. Res., 32, 2989–3001.

914 Palcsu L., Major Z., Kőllő Z. & Papp L. (2010): Using an ultrapure 4He spike in tritium measurements
915 of environmental water samples by the 3He-ingrowth method. Rapid Commun. Mass Spectrom., 24,
916 698-704.

917 Patrčević, V. (1995) Hydrological analysis of vertical water balance of groundwater at the area of
918 river alluvium. PhD thesis (in Croatian), University of Zagreb, p. 161.

919 Romić, D., Husnjak, S., Mesić, M., Salajpal, K., Barić, K., Poljak, M., Romić, M., Konjačić, M.,
920 Vnučec, I., Bakić, H., Bubalo, M., Zovko, M., Matijević, L., Lončarić, Z., Kušan, V., Brkić, Ž. &
921 Larva, O. (2014): The impact of agriculture on surface and groundwater pollution in the Republic of
922 Croatia. Faculty of Agriculture, University of Zagreb, p. 302.

923 Schlosser, P., Stute, M., Dorr, H., Sonntag, C. & Munnich, K.O. (1988): Tritium-3He dating of
924 shallow groundwater. Earth Planet. Sci. Lett., 89, 353–362.

925 Schlosser, P., Stute, M., Sonntag, C. & Munnich, K. O. (1989): Tritiogenic 3He in shallow
926 groundwater. Earth Planet. Sci. Lett., 94, 245–256.

927 Seifert, D., Sonnenborg, T.O., Scharling, P. & Hinsby, K. (2008): Use of alternative conceptual
928 models to assess the impact of a buried valley on groundwater vulnerability. Hydrogeol. J., 16, 659-
929 674.

930 Solomon, D.K., Poreda, R.J., Schiff, S.L. & Cherry, J.A. (1992): Tritium and helium 3 as groundwater
931 age tracers in the Borden aquifer. Water Resour. Res., 28, 741-755.

Solomon, D.K., Schiff, S.L. Poreda, R.J. & Clarke, W.B. (1993): A validation of the 3H/3He method for determining groundwater recharge. Water Resour. Res., 29, 2951-2962.

Stockmarr, J., Grant, R. & Jorgensen, U. (2005): Monitoring effectiveness of the EU Nitrate Directive Action Programmes: Approach by Denmark. RIVM report.

Stouman-Jensen, L., van der Hoek, K.W., Polusen, D., Zevenbergen, J.F., Palliere, C., Lammel, J. et al. (2011): Benefits of nitrogen for food, fibre and industrial production. In: Sutton, M.A. (Eds.), European nitrogen assessment, Cambridge Univ. Press, Cambridge, UK, p. 612.

Suckow, A. (2014): The Age of Groundwater – definitions, models and why we do not need this term. Applied Geochemistry, 50, 222-230.

Šegota, T. & Filipčić, A. (1996): Climatology for geographers. Jelić, T. (Ed), Školska knjiga, Zagreb, 471 p.

Thomsen, I.K. (2005). Crop N utilization and leaching losses as affected by time and method of application of farmyard manure. Eur J Agron., 22, 1-9.

Tolstikhin, I.N. & Kamenskiy, I.L. (1969): Determination of groundwater ages by the T–3He method. Geochem. Int., 6, 810–811.

Torgersen, T., Purtschert, R., Phillips, F.M., Plummer, L.N., Sanford, W. & Suckow, A. (2013): Defining Groundwater Age. In: Suckow, A., Aggarwal, P.K., Araguas-Araguas, L.J. (Eds.), Isotope Methods for Dating Old Groundwater. IAEA, Vienna, pp. 21-32.

Urbanc, J., Krivic, J., Mali, N., Ferjan, S., T., Koroša, A., Šram, D., Mezga, K., Bizjak, M., Medić, M., Bole, Z., Lojen, S., Pintar, M., Udovč, A., Glavan, M., Kacjan-Maršić, N., Jamšek, A., Valentar, V., Zadravec, D., Pušenjak, M., Klemenčič Kosi, S. (2014): Farming opportunities in water protection areas: final project report. Geological Survey of Slovenia, 154 p., Ljubljana.

Urumović, K., Šarin, A. & Donadini, K. (1981): Groundwater balance in the river basin district Drava-Dunav for 1979-1980 (Technical report – on Croatian). Croatian Geological Survey, Zagreb.

956 Urumović, K., Duić, Ž. & Hlevnjak, B. (2002): Positive and negative influences of hydroelectric
957 plants on Drava river to groundwater quality. Conference Abstracts, 21st Conference of the Danubian
958 Countries on the Hydrological Forecasting and Hydrological Bases of Water Management,
959 Bucharest, Romania, p. 91.

960 van Grinsven, H.J.M., Bouwman, L., Cassman, K.G. & van Es, H.M., McCrackin, M.L. & Beusen,
961 A.H.W. (2015): Losses of Ammonia and Nitrate from Agriculture and Their Effect on Nitrogen
962 Recovery in the European Union and the United States between 1900 and 2050. J. Environ. Qual.,
963 44/2, 356-367. https://doi.org/10.2134/jeq2014.03.0102

964 van Grinsven, H.J.M., Tiktak, A. & Rougoor, C.W. (2016): Evaluation of the Dutch implementation
965 of the nitrates directive, the Water framework directive and the national emission ceilings directive.
966 NJAS-Wagen J Life Sc., 78, 69–84.

967 Vero, S.E., Basu, N.B., van Meter, K., Richards, K.G., Mellanderl, P.E., Healya, M.G. & Fenton, O.
968 (2018): Review: the environmental status and implications of the nitrate time lag in Europe and North
969 America. Hydrogeol. J.,26, 7- 22.

970 Visser, A. (2009) Trends in groundwater quality in relation to groundwater age, PhD thesis,
971 Netherlands Geographical Studies 384, Faculty of Geosciences, Utrecht University, Netherlands.

972 Warner, M.J. & Weiss, R.F. (1985): Solubilities of chlorofluorocarbons 11 and 12 in water and
973 seawater. Deep Sea Res. Part A Oceanogr. Res. Pap. 32/12, 1485-1497.

974 Weiss, R.F. (1968): Piggyback sampler for dissolved gas studies on sealed water samples. Deep-Sea
975 Res., 15, 695-699.

976 Wiedemeier, T.H., Swanson, M.A., Moutoux, D.E. Gordon, E.K., Wilson, J.T., Wilson, B.H.,
977 Kampbell, D.H., Haas, P.E., Miller, R.N., Hansen, J.E. & Chapelle, F.H. (1998): Technical protocol
978 for evaluating natural attenuation of chlorinated solvents in ground water. EPA/600/R-98/128, U.S.
979 Environmental Protection Agency, Office of Research and Development, Washington, D.C.

980 Wilske, C., Suckow, A., Mallast, U, Meier, C, Merchel, S., Merkel, B., Pavetich, S, Rödiger, T.,
981 Rugel, G., Sachse, A., Weise, S.M. & Siebert, C. (2020): A multi-environmental tracer study to
982 determine groundwater residence times and recharge in a structurally complex multi-aquifer system.
983 Hydrol. Earth Syst. Sci., 24, 249–267.

984 Wilson, G.B. & McNeill, G.W. (1997): Noble gas temperatures and excess air component. Appl.
985 Geochem., 12, 747-762.

986 Zaninović, K.; Gajić-Čapka, M.; Perčec Tadić, M.; Vučetić, M.; Milković, J.; Bajić, A.; Cindrić, K.;
987 Cvitan, L.; Katušin, Z.; Kaučić, D.;, Likso, T.; Lončar, E.; Lončar, Ž.; Mihajlović, D.; Pandžić, K.;
988 Patarčić, M.; Srnec, L.; Vučetić, V. (2008): Klimatski atlas Hrvatske/Climate atlas of Croatia 1961–
989 1990, 1971–2000. State Hydrometeorological Institute, Zagreb, Croatia.
990 https://klima.hr/razno/publikacije/klimatski_atlas_hrvatske.pdf

991 Zheng, C. & Wang, P.P. (1999): MT3DMS: a modular three-dimensional multispecies model for
992 simulation of advection, dispersion and chemical reactions of contaminants in groundwater systems;
993 Documentation and User Guide, Contract Report SERDP-99-1, U.S. Army Engineer Research and
994 Development Center, Vicksburg, Mississippi.

995 Zoellmann, K., Kinzelbach, W. & Fuld, C. (2001): Environmental tracer transport (3H and SF6) in
996 the saturated and unsaturated zones and its use in nitrate pollution management. J. Hydrol., 240, 187–
997 205.

Figure captions

Fig. 1. Study area with hydraulic head equipotential lines and groundwater sampling locations (according to Larva, 2008)

Fig. 2. Lithological cross-section of the aquifer system (according to Larva, 2008)

Fig. 3. Flowchart of the study

Fig 4. Simulated groundwater heads for average hydrological conditions and spatial distribution of initial concentrations of nitrates in groundwater in the upper aquifer

Fig. 5. Spatial distribution of modelled nitrate concentrations in infiltrating water

Fig. 6. Nitrate concentration in groundwater in the catchment area of the Varaždin pumping site: (a) pumping wells with screen in the upper aquifer, (b) observation wells with screen in the upper aquifer, (c) mean annual nitrate concentrations (the upper aquifer), and (d) mean annual nitrate concentrations (the lower aquifer).

Fig. 7. Nitrate concentration in groundwater in the catchment area of the Bartolovec pumping site: (a) pumping and observation wells with screen in the upper aquifer, (b) pumping and observation wells with screen in the lower aquifer, (c) mean annual nitrate concentrations in both aquifers.

Fig. 8. Modelled groundwater age distribution in the sample PDS-5: (a) fraction of sample and (b) cumulative frequency

Fig. 9. Modelled groundwater age distribution in the sample BVP-3P: (a) fraction of sample and (b) cumulative frequency

Fig. 10. Modelled groundwater age distribution in the sample BVP-3D: (a) fraction of sample and (b) cumulative frequency

Fig. 11. Input data on agricultural N: (a) consumption of fertilizers in the EU and Croatia and (b) input data on N fertilizer, N manure and N surplus in EU (http://www.fao.org/faostat/en/#data/EF).

Fig. 12. Time series of the mineral fertilizer consumption according to Romić et al. (2014) and mean annual nitrate concentrations in groundwater in the wider area of the Varaždin pumping site

Fig. 13. Time series of the mineral fertilizer consumption in the Varaždin area according to Grđan et al. (1991) and mean annual nitrate concentration in groundwater in the area of Varaždin pumping site

Fig. 14. Time series of the mineral fertilizer consumption according to Romić et al. (2014) and mean annual nitrate concentrations in groundwater at the Bartolovec pumping site

Fig. 15. Simulated and observed nitrate concentrations at observation wells PDS-5 (a), PDS-6 (b) and PDS-7 (c) at the Varaždin pumping site

Fig. 16. Simulated and observed nitrate concentrations in the upper (a) and lower aquifer (b) at the Bartolovec pumping site

Figure 1

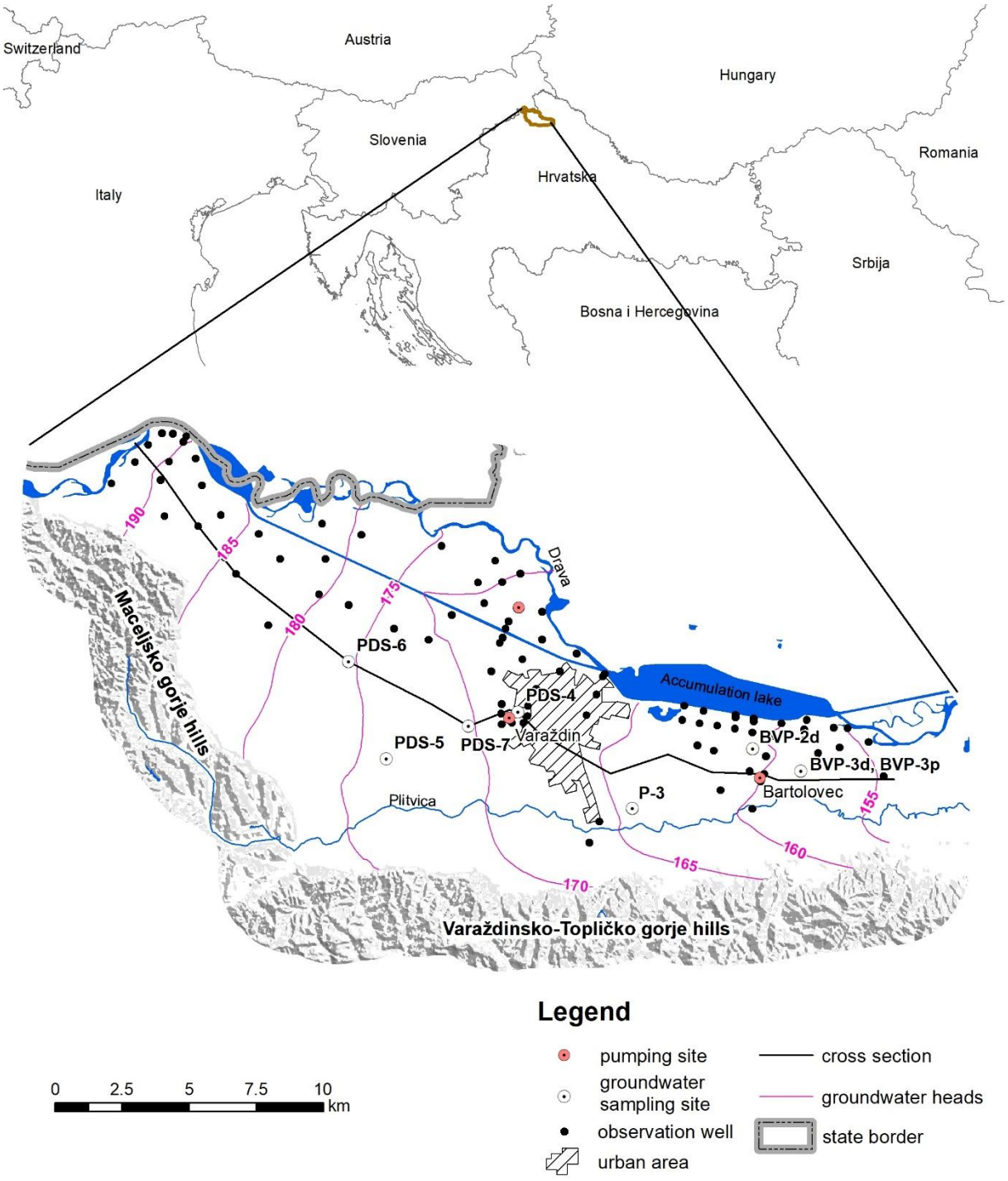
Switzerland
Austria
Hungary
Slovenia
Romania
Italy
Hrvatska
Srbija
Bosna i Hercegovina
190
185
180
175
Drava
Macelj'sko gorje hills
PDS-6
PDS-4
Accumulation lake
PDS-5
PDS-7
Varaždin
BVP-2d
BVP-3d, BVP-3p
Bartolovec
P-3
Plitvica
155
160
165
170
Varaždinsko-Topličko gorje hills
0 2.5 5 7.5 10 km
Legend
pumping site
groundwater sampling site
observation well
urban area
cross section
groundwater heads
state border

Figure 2

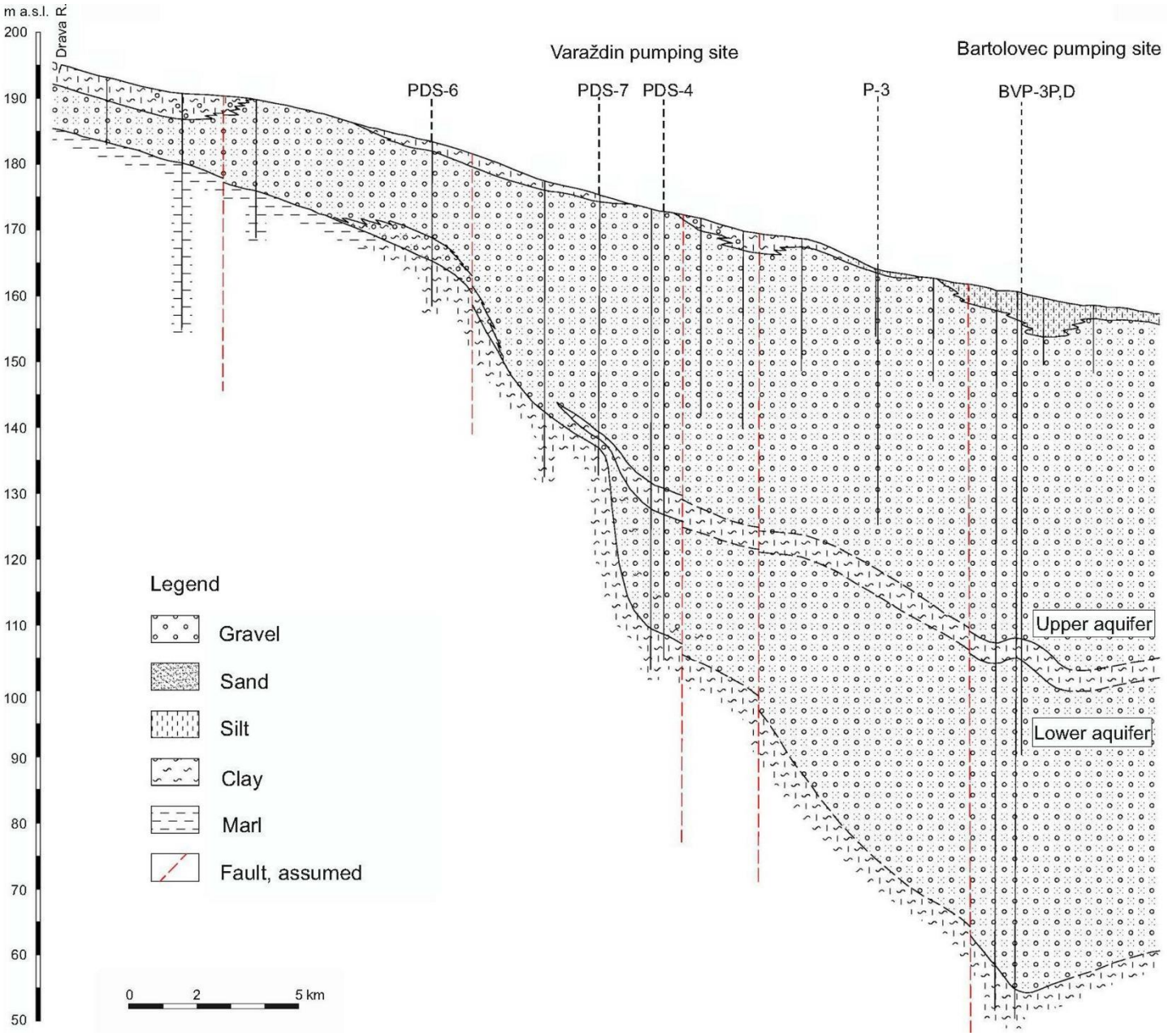
m a.s.l.
Drava R.
200
190
180
170
160
150
140
130
120
110
100
90
80
70
60
50
Varaždin pumping site
Bartolovec pumping site
PDS-6
PDS-7
PDS-4
P-3
BVP-3P,D
Upper aquifer
Lower aquifer
Legend
Gravel
Sand
Silt
Clay
Marl
Fault, assumed
0
2
5 km

Figure 3

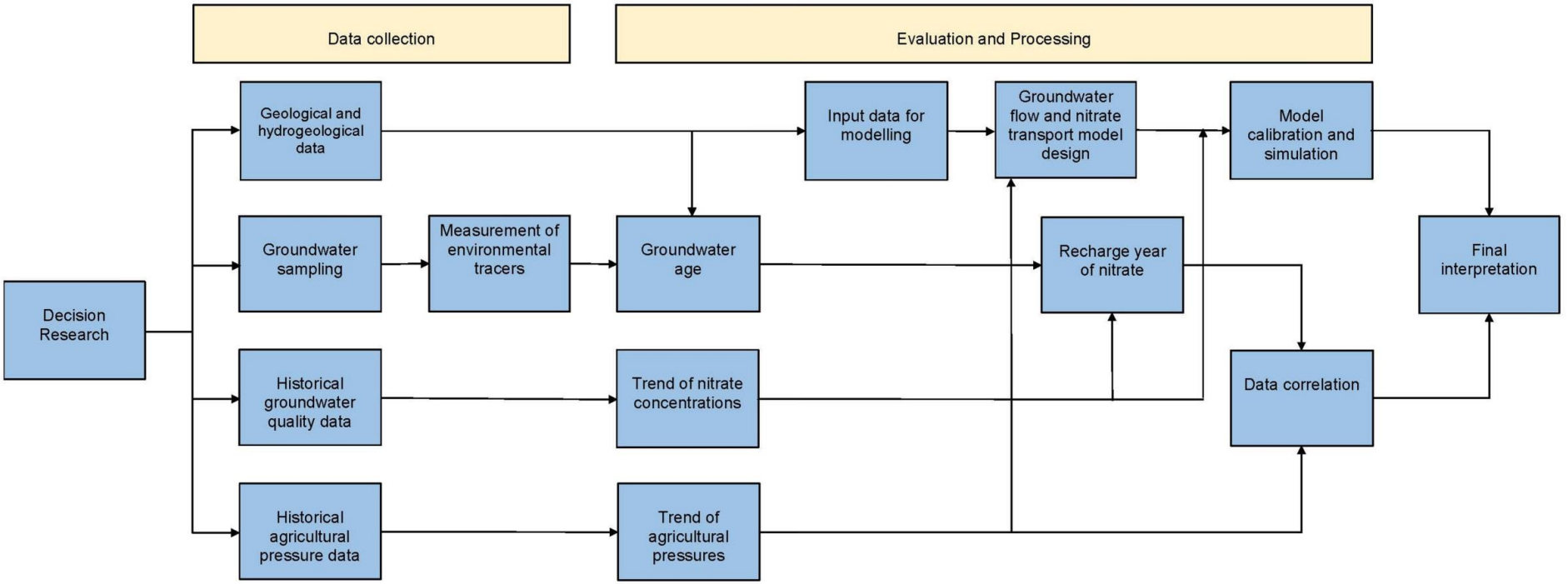
Data collection
Evaluation and Processing
Geological and hydrogeological data
Input data for modelling
Groundwater flow and nitrate transport model design
Model calibration and simulation
Groundwater sampling
Measurement of environmental tracers
Groundwater age
Recharge year of nitrate
Final interpretation
Decision Research
Historical groundwater quality data
Trend of nitrate concentrations
Data correlation
Historical agricultural pressure data
Trend of agricultural pressures

Figure 4

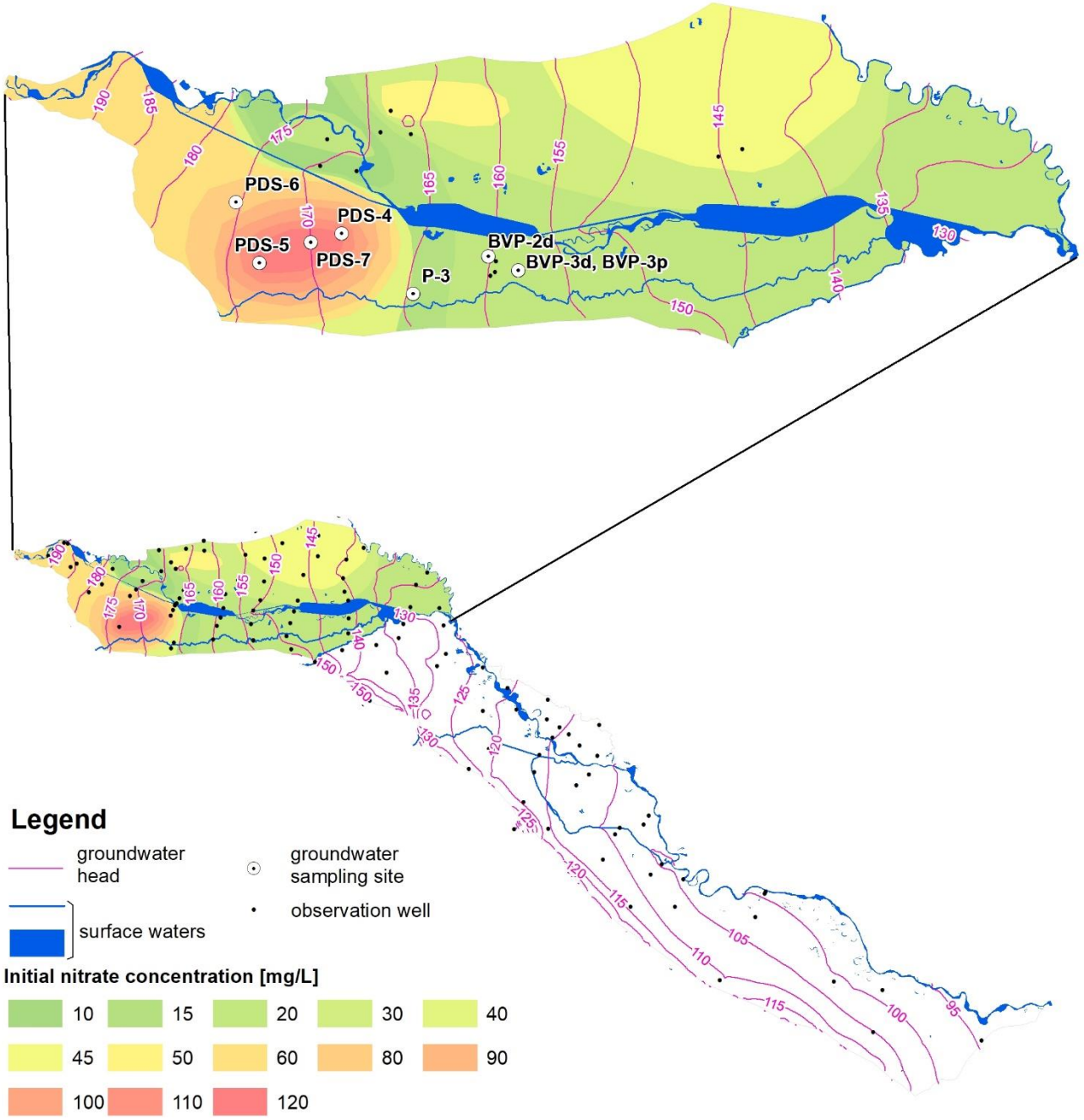
PDS-6
PDS-4
PDS-5
PDS-7
P-3
BVP-2d
BVP-3d, BVP-3p
Legend
groundwater head
groundwater sampling site
observation well
surface waters
Initial nitrate concentration [mg/L]
10
15
20
30
40
45
50
60
80
90
100
110
120

Figure 5

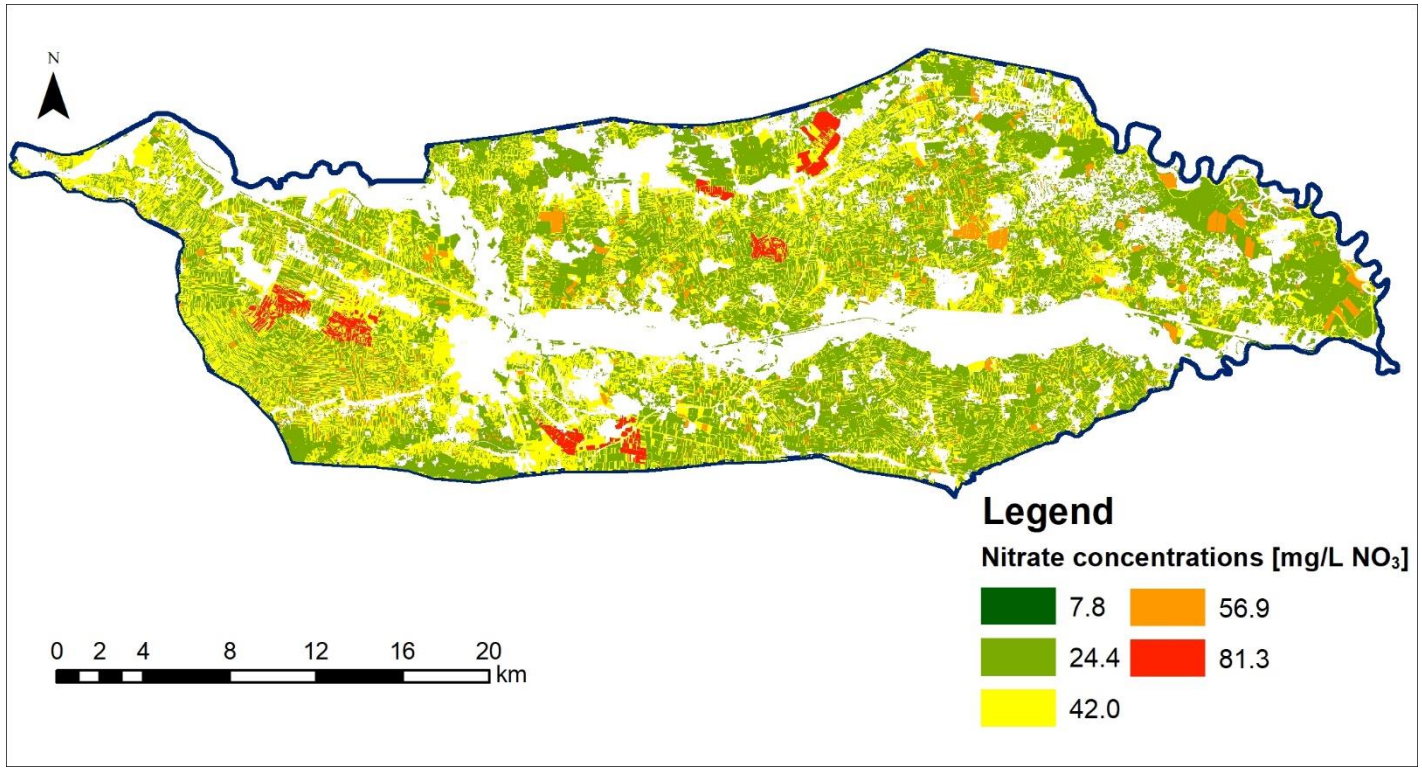
N
0 2 4 8 12 16 20
km
Legend
Nitrate concentrations [mg/L NO3]
7.8
24.4
42.0
56.9
81.3

Figure 6

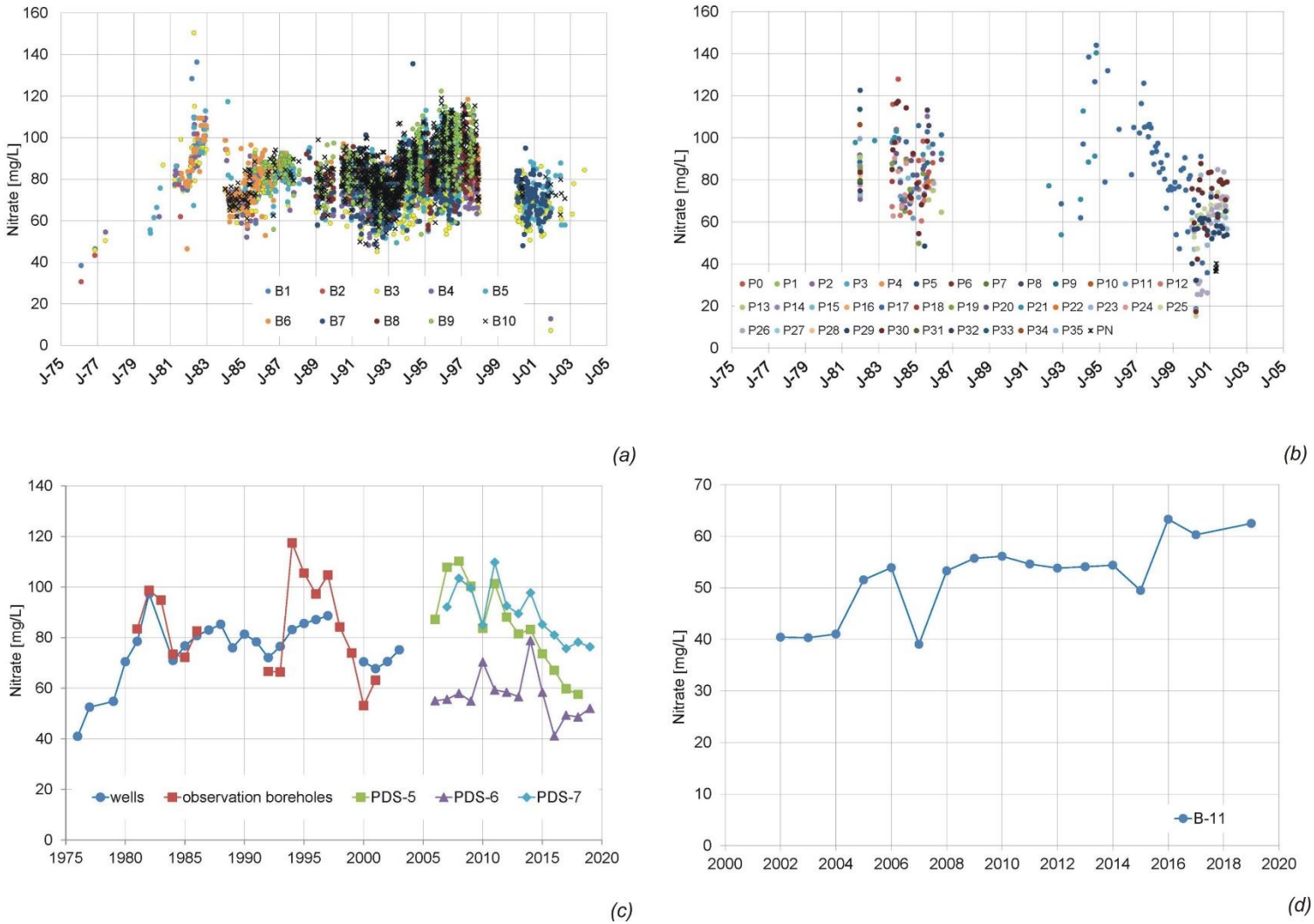
Nitrate [mg/L]
B1 B2 B3 B4 B5
B6 B7 B8 B9 B10
(a)
P0 P1 P2 P3 P4 P5 P6 P7 P8 P9 P10 P11 P12
P13 P14 P15 P16 P17 P18 P19 P20 P21 P22 P23 P24 P25
P26 P27 P28 P29 P30 P31 P32 P33 P34 P35 PN
(b)
wells observation boreholes PDS-5 PDS-6 PDS-7
(c)
B-11
(d)

Figure 7

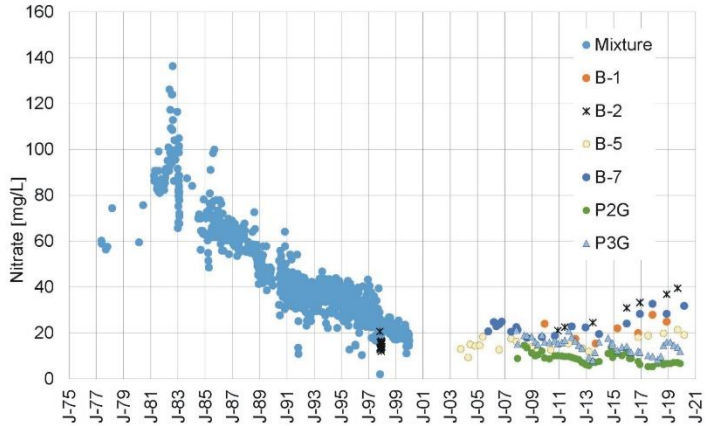
Nitrate [mg/L]
Mixture
B-1
B-2
B-5
B-7
P2G
P3G

(a)

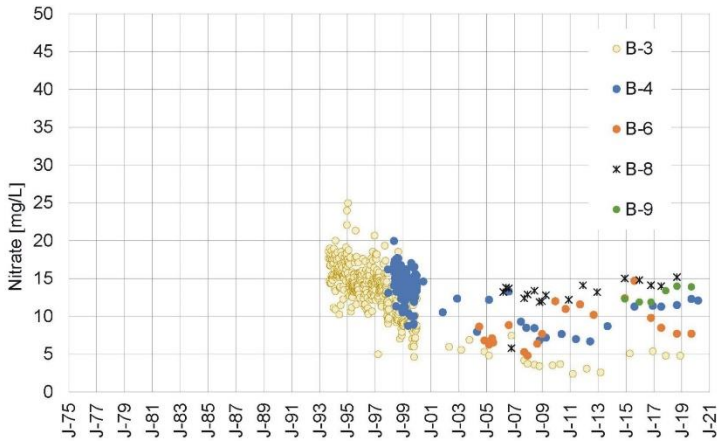
Nitrate [mg/L]
B-3
B-4
B-6
B-8
B-9

(b)

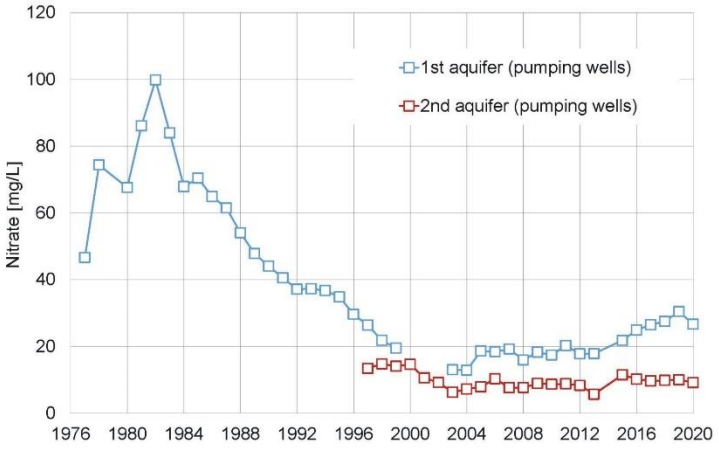
Nitrate [mg/L]
1st aquifer (pumping wells)
2nd aquifer (pumping wells)

(c)

Figure 8

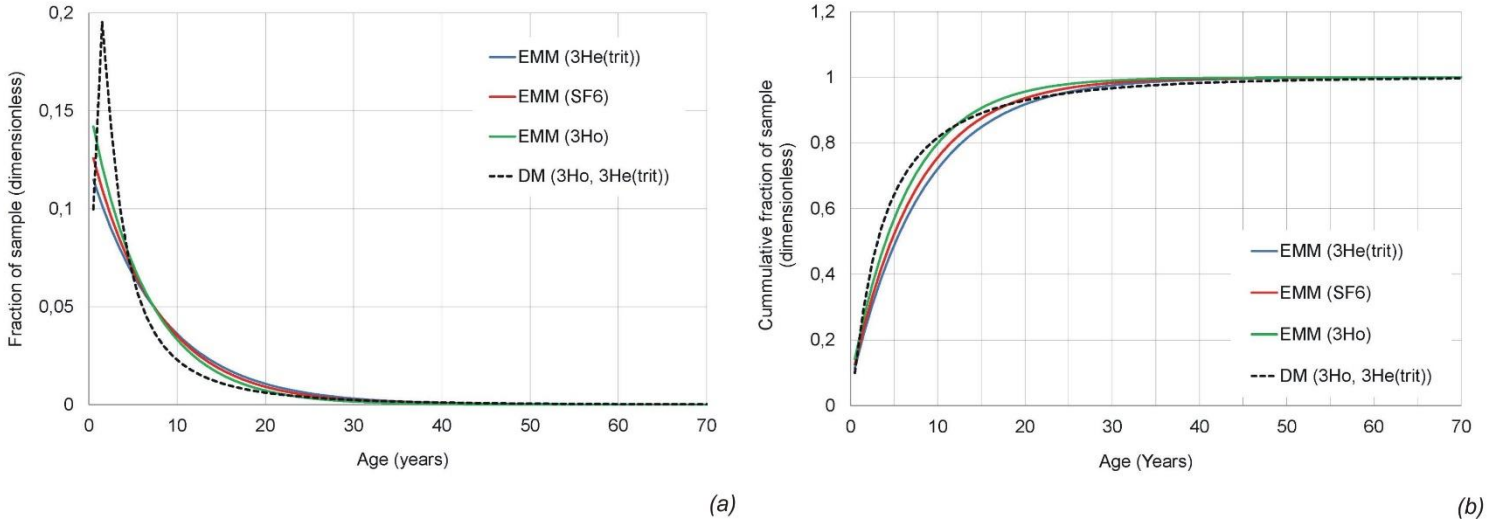
0,2
0,15
0,1
0,05
0
Fraction of sample (dimensionless)
0
10
20
30
40
50
60
70
Age (years)
EMM (3He(trit))
EMM (SF6)
EMM (3Ho)
DM (3Ho, 3He(trit))
1,2
1
0,8
0,6
0,4
0,2
0
Cummulative fraction of sample (dimensionless)
Age (Years)
EMM (3He(trit))
EMM (SF6)
EMM (3Ho)
DM (3Ho, 3He(trit))

(a) *(b)*

Figure 9

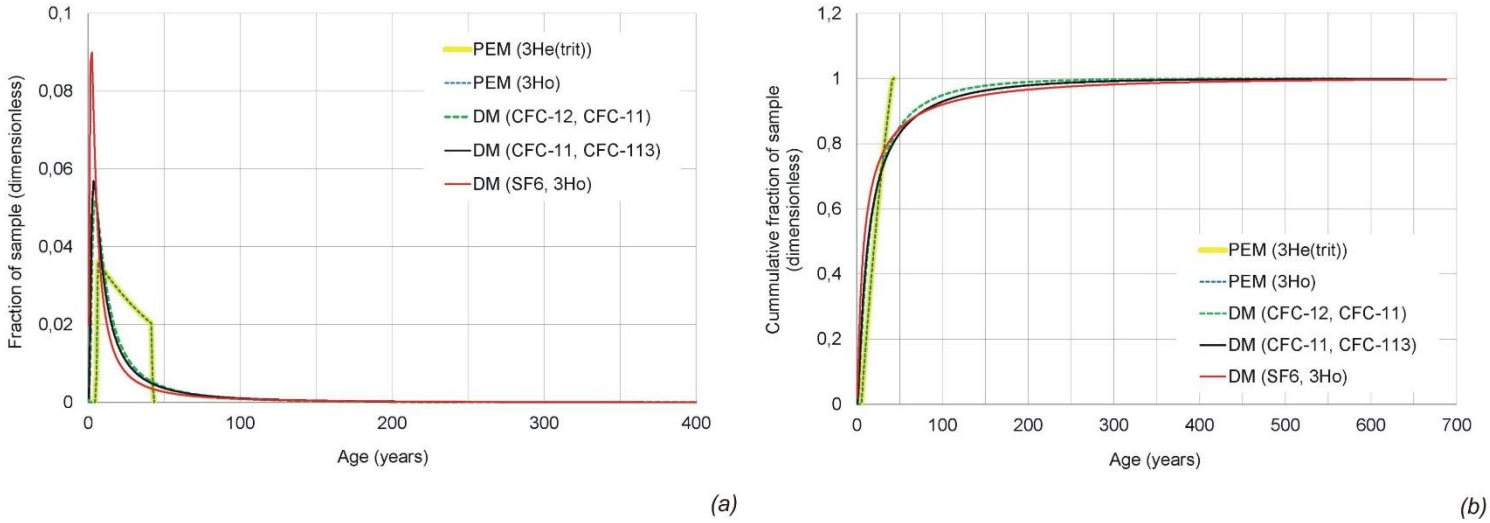
0,1
0,08
0,06
0,04
0,02
0
Fraction of sample (dimensionless)
0
100
200
300
400
Age (years)
PEM (3He(trit))
PEM (3Ho)
DM (CFC-12, CFC-11)
DM (CFC-11, CFC-113)
DM (SF6, 3Ho)
(a)
1,2
1
0,8
0,6
0,4
0,2
0
Cummulative fraction of sample (dimensionless)
0
100
200
300
400
500
600
700
Age (years)
PEM (3He(trit))
PEM (3Ho)
DM (CFC-12, CFC-11)
DM (CFC-11, CFC-113)
DM (SF6, 3Ho)
(b)

Figure 10

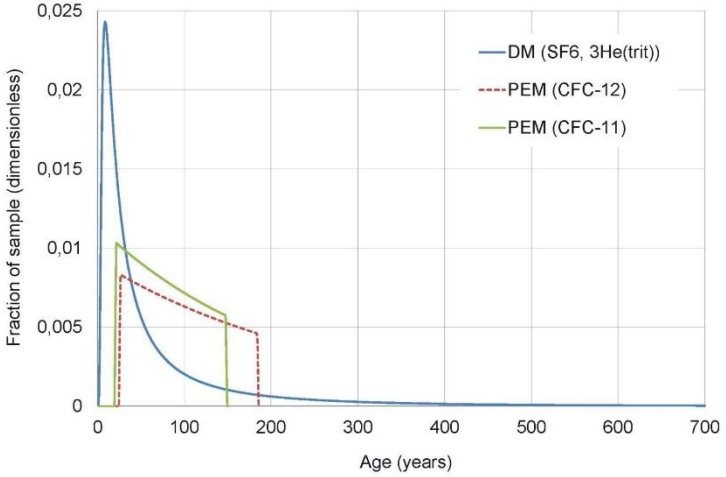
0,025
0,02
0,015
0,01
0,005
0
Fraction of sample (dimensionless)
0
100
200
300
400
500
600
700
Age (years)
DM (SF6, 3He(trit))
PEM (CFC-12)
PEM (CFC-11)

(a)

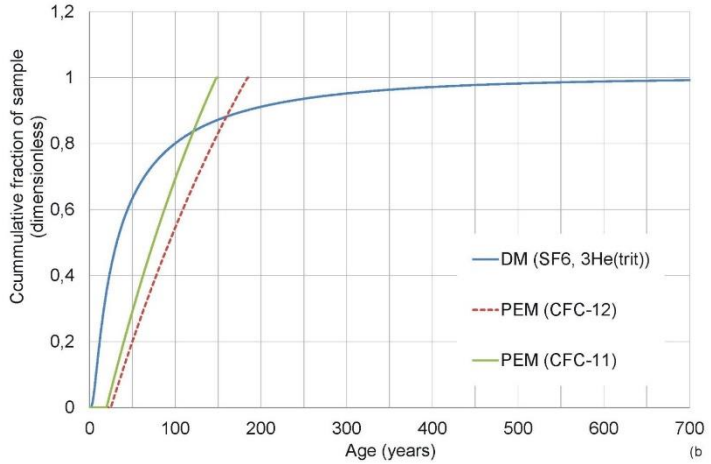
1,2
1
0,8
0,6
0,4
0,2
0
Ccummulative fraction of sample (dimensionless)
0
100
200
300
400
500
600
700
Age (years)
DM (SF6, 3He(trit))
PEM (CFC-12)
PEM (CFC-11)

(b

Figure 11

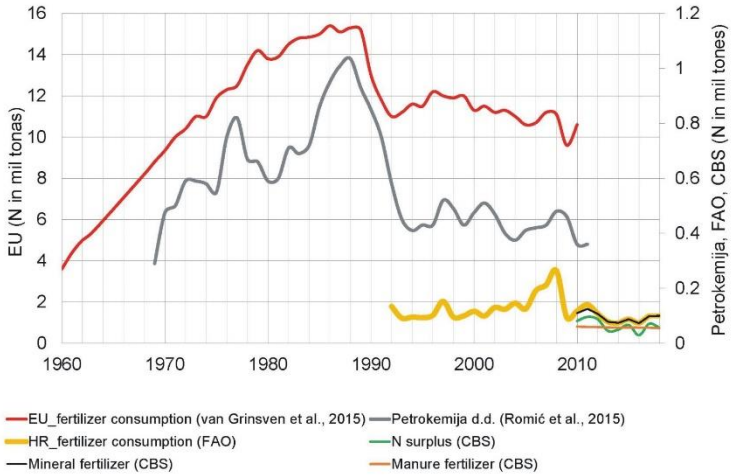
EU (N in mil tonas)
Petrokemija, FAO, CBS (N in mil tones)
EU_fertilizer consumption (van Grinsven et al., 2015)
Petrokemija d.d. (Romić et al., 2015)
HR_fertilizer consumption (FAO)
N surplus (CBS)
Mineral fertilizer (CBS)
Manure fertilizer (CBS)

(a)

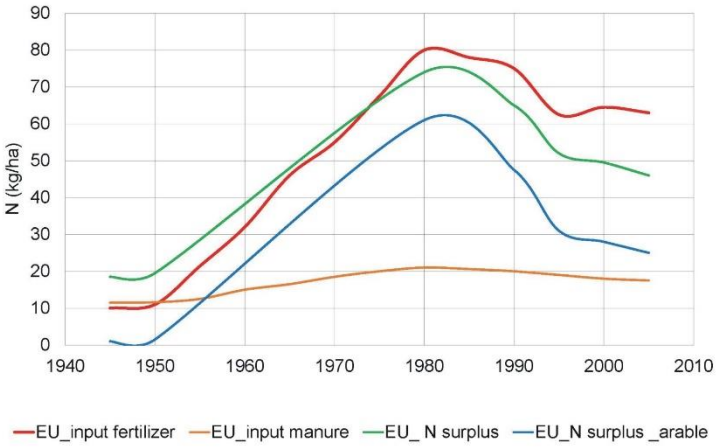
N (kg/ha)
EU_input fertilizer
EU_input manure
EU_ N surplus
EU_N surplus _arable

(b)

Figure 12

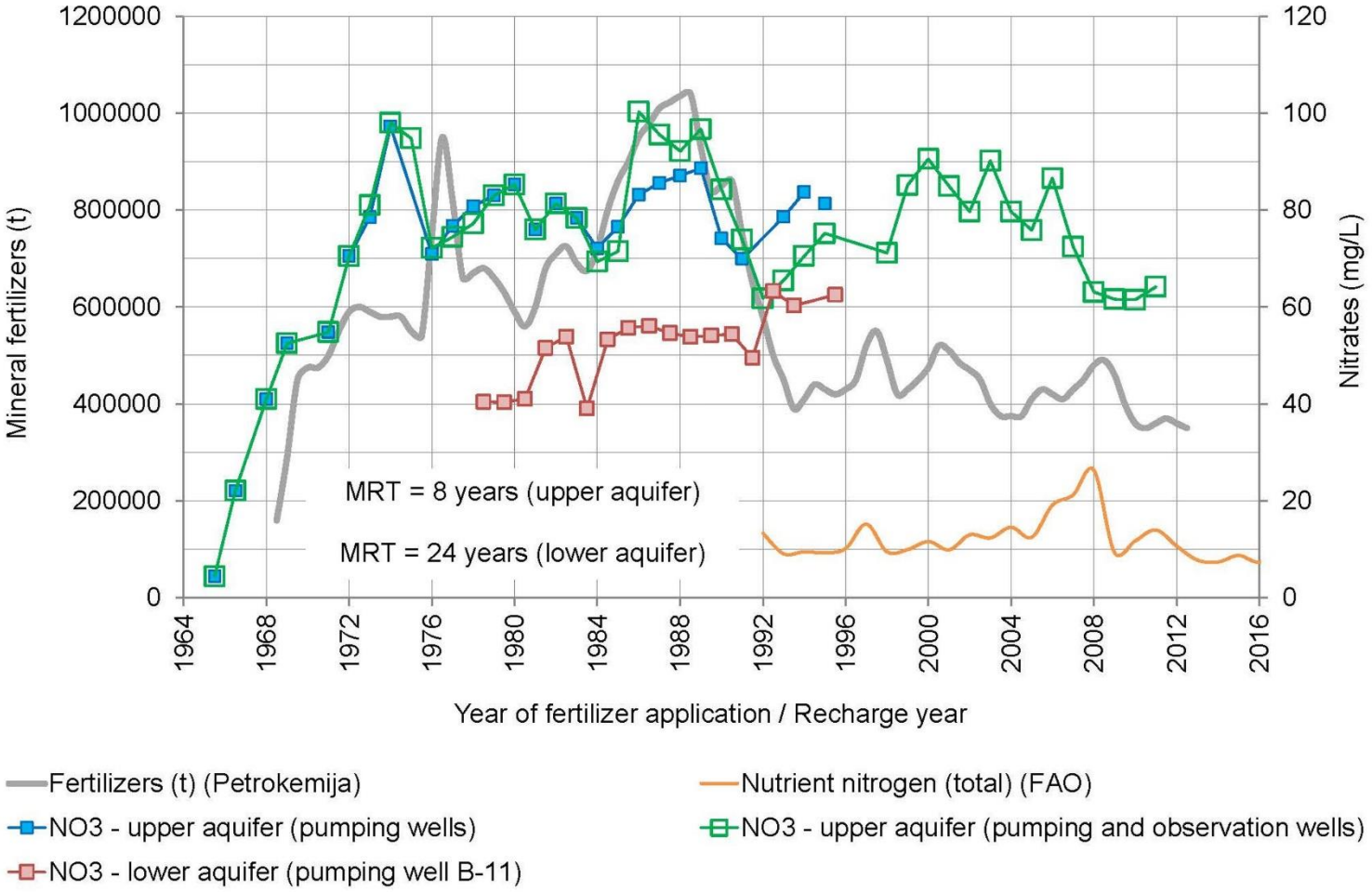
1200000
1000000
800000
600000
400000
200000
0
120
100
80
60
40
20
0
Mineral fertilizers (t)
Nitrates (mg/L)
1964
1968
1972
1976
1980
1984
1988
1992
1996
2000
2004
2008
2012
2016
MRT = 8 years (upper aquifer)
MRT = 24 years (lower aquifer)
Year of fertilizer application / Recharge year
Fertilizers (t) (Petrokemija)
Nutrient nitrogen (total) (FAO)
NO3 - upper aquifer (pumping wells)
NO3 - upper aquifer (pumping and observation wells)
NO3 - lower aquifer (pumping well B-11)

Figure 13

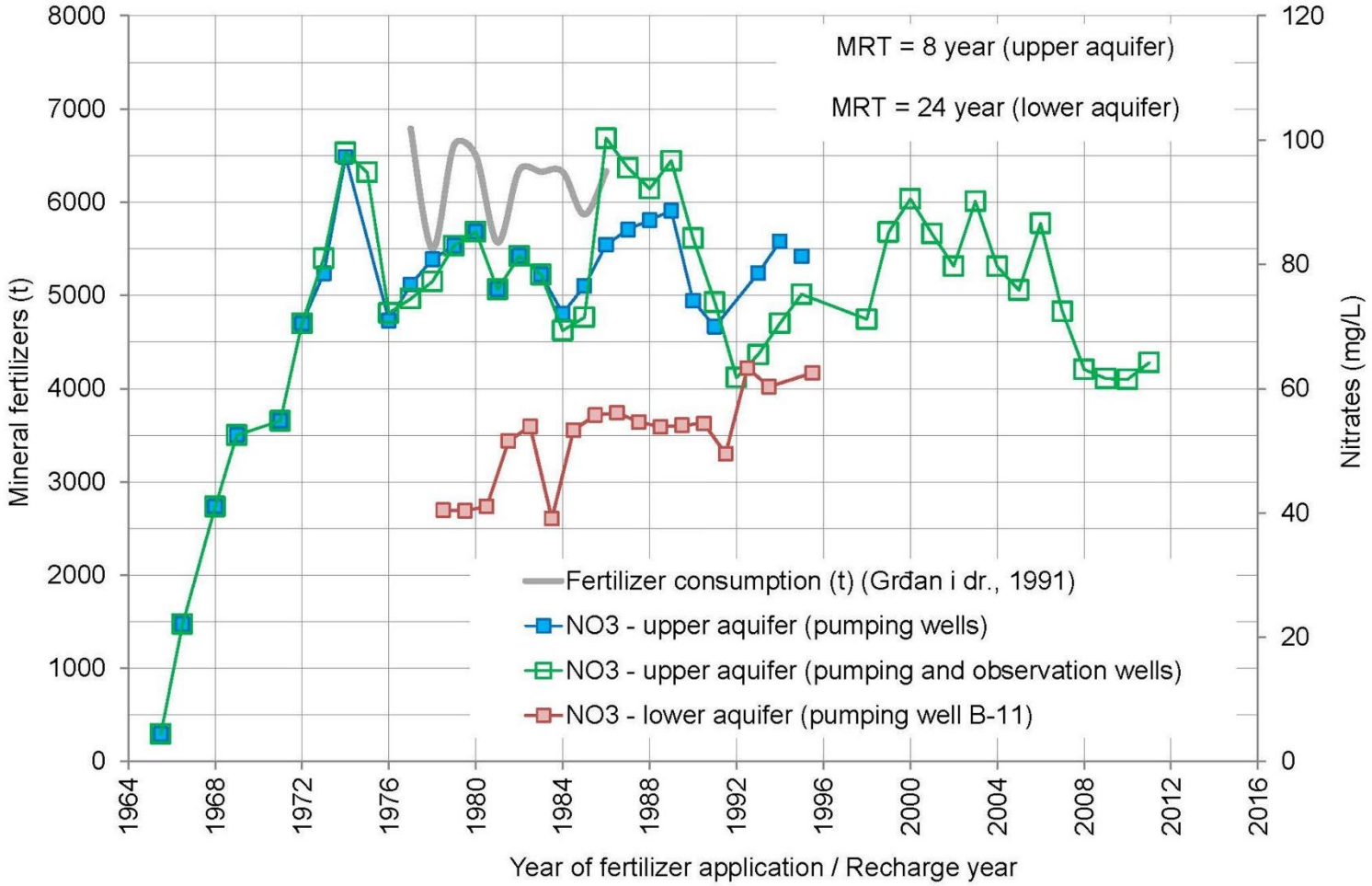
MRT = 8 year (upper aquifer)
MRT = 24 year (lower aquifer)
Fertilizer consumption (t) (Grđan i dr., 1991)
NO3 - upper aquifer (pumping wells)
NO3 - upper aquifer (pumping and observation wells)
NO3 - lower aquifer (pumping well B-11)
Mineral fertilizers (t)
Nitrates (mg/L)
Year of fertilizer application / Recharge year
0
1000
2000
3000
4000
5000
6000
7000
8000
0
20
40
60
80
100
120
1964
1968
1972
1976
1980
1984
1988
1992
1996
2000
2004
2008
2012
2016

Figure 14

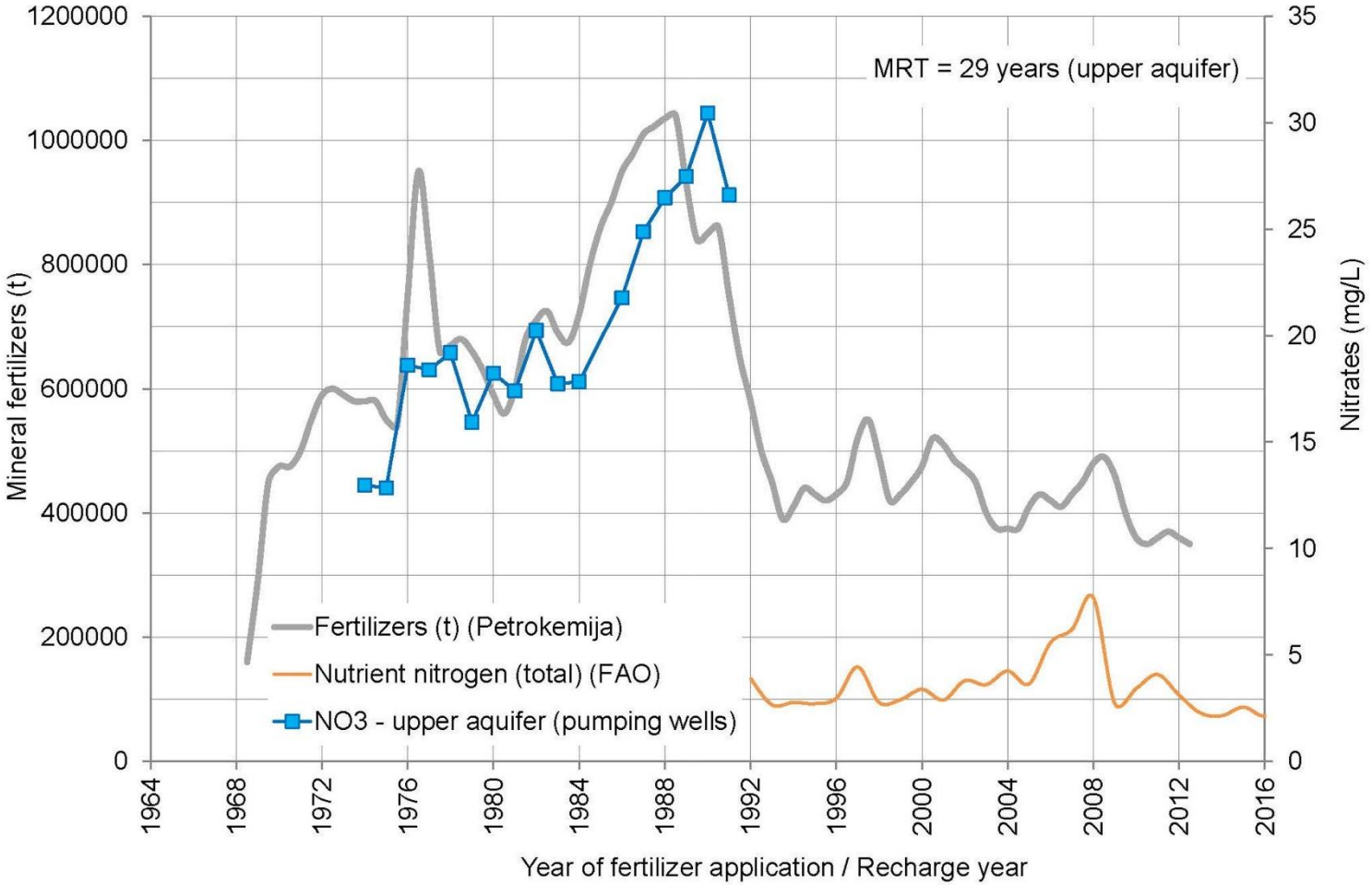
MRT = 29 years (upper aquifer)
Mineral fertilizers (t)
Nitrates (mg/L)
Year of fertilizer application / Recharge year
Fertilizers (t) (Petrokemija)
Nutrient nitrogen (total) (FAO)
NO3 - upper aquifer (pumping wells)
1200000
1000000
800000
600000
400000
200000
0
35
30
25
20
15
10
5
0
1964
1968
1972
1976
1980
1984
1988
1992
1996
2000
2004
2008
2012
2016

Figure 15

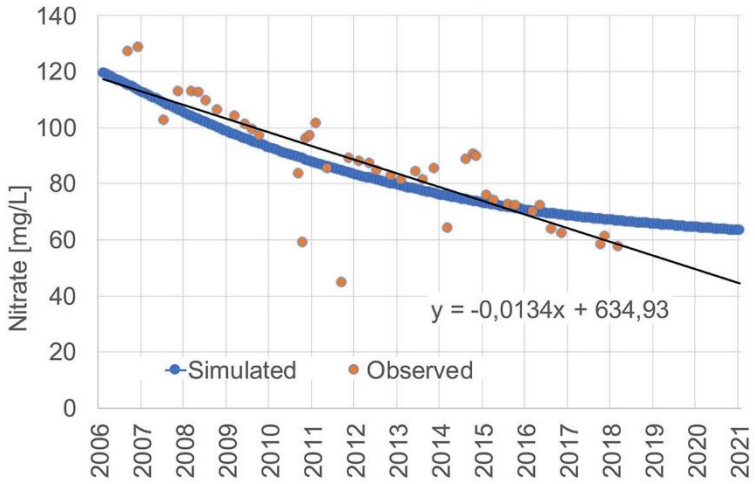

a)

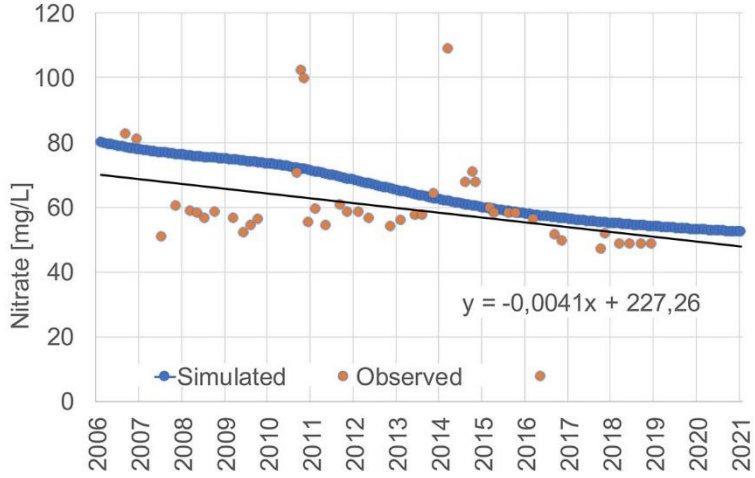

b)

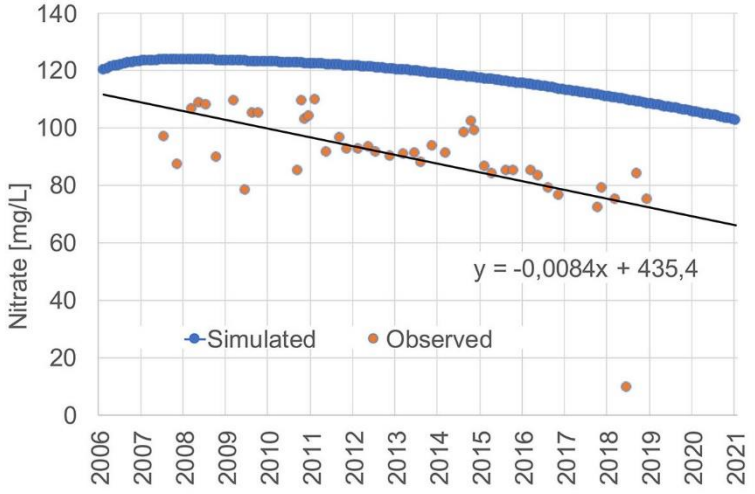

c)

Figure 16

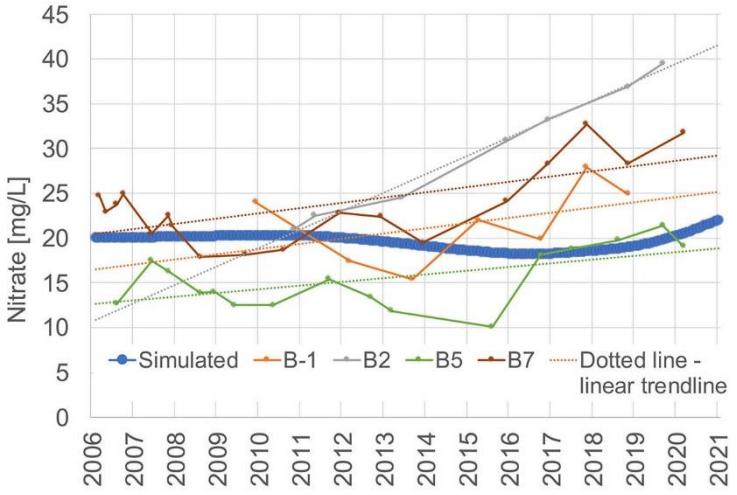
Nitrate [mg/L]
45
40
35
30
25
20
15
10
5
0
Simulated
B-1
B2
B5
B7
Dotted line - linear trendline
2006
2007
2008
2009
2010
2011
2012
2013
2014
2015
2016
2017
2018
2019
2020
2021

a)

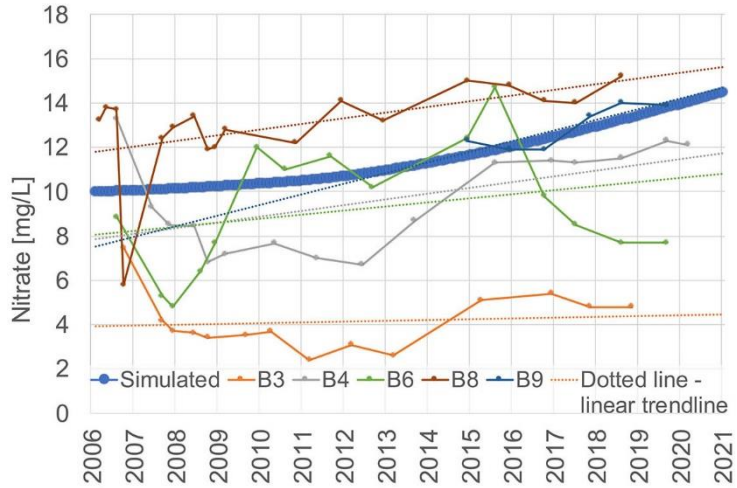
Nitrate [mg/L]
18
16
14
12
10
8
6
4
2
0
Simulated
B3
B4
B6
B8
B9
Dotted line - linear trendline
2006
2007
2008
2009
2010
2011
2012
2013
2014
2015
2016
2017
2018
2019
2020
2021

b)

Table 1. Characteristics of groundwater sampling sites

Observation borehole	Recharge elevation (m a.s.l)	Annual mean air temperature* (°C) 1960-1991/1971-2000	Depth of unsaturated zone (m)	Sampling date ($^3H/^3He$ and CFCs)	Borehole depth (m)	Screen interval	Sampling depth (m)
PDS-5	170-200	9.9/10.2	2-6	11, 2017 and 03, 2018	26.0	13.7-19.7	15
PDS-6				11, 2017 and 03, 2018	24.0	11.7-17.7	15
PDS-7				11, 2017 and 03, 2018	34.0	29.3-32.3	15
PDS-4				11, 2019 and 03, 2020	66.7	42.0-46.0, 48.7-60.7	58
P-3D				11, 2019 and 03, 2020	40.0	4.0-19.0, 22.0-37.0	35
BVP-2D				11, 2019 and 03, 2020	71.0	57.0-69.0	50
BVP-3P				11, 2019 and 03, 2020	40.0	27.0-39.0	30
BVP-3D				11, 2019 and 03, 2020	70.0	58.0-70.0	58

* Zaninović et al. (2008)

Table 2. Nitrate concentration data sets used to analyze the impact of agricultural pressures on groundwater

Observation borehole	Data time series	Data source
PDS-5		
PDS-6	2006-2019	Hrvatske vode (a legal entity for water management in Croatia)
PDS-7		
Wells and observation boreholes at the Varaždin and Bartolovec pumping sites	1973-2019	Varkom Ltd. for water supply and wastewater drainage (Varaždin)

Table 3. Agricultural lands and nitrate concentrations

Crop	Agricultural land use classes	Nitrate concentration in infiltrating water [mg/L NO_3]
Tobacco	Non-intensive land use	7.8
Cereals, corn, sugar beet, soy, oilseeds, potato, vineyards, meadows, pastures, sunflower	Extensive land use	24.4
Mosaic	A combination of extensive and intensive land use	42.0
Vegetables, cabbage, orchards	Intensive land use	56.9
Agricultural land in vicinity of farms	Nitrate on farmland	81.3

Table 4 Tracer concentrations in groundwater

Sample name	CFC conc. (pmol/L)			SF_6 (fmol/L)	^3H (TU)	^3H error (TU)	$^3H+^3He_{trit}$ (TU)	$^3H+^3He_{trit}$ error (TU)
	CFC-12	CFC-11	CFC-113					
PDS-5	**3.3 ± 0.2**	**10 ± 2**	0.42 ± 0.05	3.3 ± 0.4	4.91	0.09	10.6	0.9
PDS-6	**4.1 ± 0.3**	**19 ± 4**	0.43 ± 0.05	3.3 ± 0.4	5.05	0.09	7.9	0.8
PDS-7	**3.2 ± 0.2**	**10 ± 2**	0.43 ± 0.05	3.0 ± 0.3				
PDS-4	**3.3 ± 0.2**	**13 ± 3**	0.46 ± 0.05	1.6 ± 0.2	4.06	0.08	23.1	1.2
P-3D	**10 ± 3**	**30 ± 10**	0.34 ± 0.05	2.6 ± 0.3	4.90	0.18	27.2	1.4
BVP-2D	0.65 ± 0.05	0.8 ± 0.1	0.15 ± 0.05	2.2 ± 0.3				
BVP-3P	2.1 ± 0.2	5.3 ± 0.6	0.23 ± 0.05	3.4 ± 0.4	4.43	0.18	17.3	1.1
BVP-3D	0.42 ± 0.05	1.3 ± 0.2	0.04 ± 0.05	1.3 ± 0.2	1.63	0.06	53.5	2.0

Table 5. Calculated travel time range for groundwater samples and comparison with the calculated MRT using the environmental tracers

Sample name	Sampling depth below water table (m)	Recharge rate (mm/year)	Porosity (dimensionless)	Travel time (years)	MRT defined by the environmental tracers (years)
PDS-5	12	200-300	0.23	9.2 - 13.8	(29)* 6.5 - 13.7
PDS-6	9			6.9 - 10.4	(29)* 6.5 - 8.0
PDS-7	10			7.7 - 11.5	(29)* 9.0
PDS-4	49			37.6 - 56.4	24.5 - 30.9
P-3D	33			25.3 - 38.0	(14.5)** 30.4 - 33.0
BVP-2D	44			33.7 - 50.6	(18.5)** 39.5 - 53.0
BVP-3P	27			20.7 - 31.1	(7.5)** 24.2 - 36.0
BVP-3D	53			40.6 - 61.0	(27.5)** 49 - 62.1

* (MRT defined using CFC-113)
** (MRT defined using SF_6)

Table 6 Summary of modelled MRTs extracted from different tracer combinations. PM: piston flow model; EMM: exponential mixing model; PEM: partial exponential model; DM: dispersion model.

Sample name	LPM	MRT (years)	Error (years)	Modeled tracer	Mean value of MRT (years)
PDS-5	EMM	8.2	0.5	$^{3}He(trit)$	8
PDS-5	EMM	6.5	1.3	$^{3}H_0$	
PDS-5	DM	7.0	0.03	$^{3}H_0$, $^{3}He(trit)$	
PDS-6	EMM	6.8	1.1	$^{3}He(trit)$	
PDS-6	DM	9.4	0.03	$^{3}H_0$, $^{3}He(trit)$	
BVP-3P	PEM	22.2	0.4	$^{3}He(trit)$	29
BVP-3P	PEM	22.2	0.6	$^{3}H_0$	
BVP-3P	DM	28.4	0.3	CFC-12, CFC-11	
BVP-3P	DM	32.3	0.3	CFC-11, CFC-113	
BVP-3P	DM	34.3	0.0	SF_6, $^{3}H_0$	
BVP-2D	DM	69.7	0.3	CFC-12, CFC-113	
PDS-4	PEM	25.3	2.8	SF_6	24
PDS-4	PEM	24.0	0.3	$^{3}He(trit)$	
PDS-4	PEM	23.9	0.5	$^{3}H_0$	
BVP-3D	PEM	78.1	6.8	CFC-11	84
BVP-3D	PEM	97.2	4.9	CFC-12	
BVP-3D	DM	75.6	9.5	SF_6, $^{3}He(trit)$	